

Ruby Joint Stabilization System as a Suitable Method of Extracapsular Repair

Christopher G. Dominic

Thesis submitted to the faculty of the Virginia Polytechnic Institute and State University  
in partial fulfillment of the requirements for the degree of

Master of Science  
In  
Biomedical and Veterinary Science

Otto I. Lanz, Committee Chair  
Dominique M. Sawyere  
Noelle M. Muro  
Theresa E. Pancotto

5/27/2021  
Blacksburg, VA

Keywords: Cranial Cruciate Ligament, Ruby, Canine, Stifle, Extracapsular

# Ruby Joint Stabilization System<sup>a</sup> as a Suitable Method of Extracapsular Repair

Christopher G. Dominic

## 1 ABSTRACT

**Objective:** To characterize the effect of the Ruby Joint Stabilization System (Ruby) on the motion of the cranial cruciate ligament (CrCL) deficient stifle. To compare the motion with the Ruby to that of the CrCL-intact and CrCL-deficient stifle.

**Study Design:** Each canine pelvic limb was mounted in a loading jig under 30% body weight. Motion data was collected using an electromagnetic tracking system at stifle angles of 125°, 135° and 145° with the CrCL-intact, CrCL-deficient and the Ruby applied.

**Results:** Total translation of the CrCL-deficient stifle following the Ruby was reduced, but remained greater than the CrCL-intact stifle at angles of 125°, 135° and 145°. Internal rotation of the Ruby groups was greater than the CrCL-intact group at 145°, but not 125° and 135°. Varus motion of the Ruby group was decreased compared to the CrCL-deficient group, but increased compared to the CrCL-intact group at angles of 125°, 135° and 145°.

**Conclusion:** Total translation and internal rotation of the CrCL-deficient stifle following the Ruby differed from that of the CrCL-intact stifle. However, the Ruby reduced total translation and internal rotation of the tibia relative to the femur in the CrCL-deficient stifle to levels that may yield clinically acceptable results.

---

<sup>a</sup> KYON Veterinary Surgical Products, Zurich, Switzerland

# Ruby Joint Stabilization System as a Suitable Method of Extracapsular Repair

Christopher G. Dominic

## **2 GENERAL AUDIENCE ABSTRACT**

Cranial cruciate ligament disease is a common pathology of the canine stifle. Loss of this ligament results in instability of the stifle that results in pain and osteoarthritis, and can lead to damage of other intra-articular structures like the menisci. An abundant number of surgical procedures are described, with the goal of surgery being the restoration of normal stifle stability and function. A common surgical procedure for treatment is the lateral suture technique, which is an extracapsular method of stabilization. This procedure faces many complications; however, it remains a popular choice of stabilization due to its lower cost and less invasive nature. The Ruby Joint Stabilization procedure is a method of extracapsular repair that aims to restore stifle stability and circumvent several complications that plague the lateral suture. This cadaveric study sought to investigate how stifle motion of the normal canine stifle compared to that of the cranial cruciate ligament deficient stifle with the Ruby Joint Stabilization System applied. The results of this investigation demonstrated that the Ruby Joint Stabilization System adequately restored stifle motion to a level that could yield clinically acceptable results, as was demonstrated in a previously published clinical investigation of this technique.

### **3 ACKNOWLEDGEMENTS**

I would like to thank KYON Veterinary Surgical Products for donating a portion of the materials required for the completion of this investigation, Slobodan Tepic for his aid with the experimental design, David Seda for his assistance with the statistical analysis, and the technical support staff of Polhemus for their assistance.

## 4 TABLE OF CONTENTS

<b>1</b>	<b>ABSTRACT.....</b>	<b>ii</b>
<b>2</b>	<b>GENERAL AUDIENCE ABSTRACT.....</b>	<b>iii</b>
<b>3</b>	<b>ACKNOWLEDGEMENTS .....</b>	<b>iv</b>
<b>4</b>	<b>TABLE OF CONTENTS .....</b>	<b>v</b>
<b>5</b>	<b>ATTRIBUTION .....</b>	<b>vii</b>
<b>6</b>	<b>CHAPTER I: LITERATURE REVIEW .....</b>	<b>1</b>
<b>6.1</b>	<b>Canine Stifle Anatomy.....</b>	<b>1</b>
6.1.1	Joint:.....	1
6.1.2	Bones: .....	1
6.1.3	Joint Capsule:.....	2
6.1.4	Musculature: .....	2
6.1.5	Vascular Supply:.....	4
6.1.6	Lymphatics:.....	6
6.1.7	Innervation: .....	7
6.1.8	Meniscus: .....	7
6.1.9	Ligaments:.....	9
<b>6.2</b>	<b>Stifle Kinematics .....</b>	<b>11</b>
6.2.1	Normal Stifle.....	11
6.2.2	The Cranial Cruciate Ligament Deficient Stifle .....	12
<b>6.3</b>	<b>Cranial Cruciate Ligament Disease .....</b>	<b>14</b>
6.3.1	Etiopathogenesis .....	14
6.3.2	Meniscal Injury .....	19
6.3.3	Osteoarthritis:.....	19
6.3.4	Diagnosis: .....	20
6.3.5	Treatment Options .....	23
<b>6.4</b>	<b>The Lateral Suture.....</b>	<b>30</b>
6.4.1	Suture Material: .....	30
6.4.2	Suture Securing Methods:.....	31
6.4.3	Isometry: .....	32
6.4.4	Complications: .....	32
<b>7</b>	<b>CHAPTER II: Ruby Joint Stabilization System as an Extracapsular Method of Repair.....</b>	<b>34</b>
<b>7.1</b>	<b>Objective:.....</b>	<b>34</b>
<b>7.2</b>	<b>Materials &amp; Methods:.....</b>	<b>34</b>
7.2.1	Specimen Collection and Preparation:.....	34
7.2.2	Radiographic Analysis:.....	34
7.2.3	Ruby Procedure:.....	34
7.2.4	Testing Protocol:.....	35
7.2.5	Data Collection: .....	36
7.2.6	Statistical Analysis:.....	36

<b>7.3</b>	<b>Results .....</b>	<b>37</b>
<b>7.4</b>	<b>Discussion .....</b>	<b>37</b>
<b>7.5</b>	<b>Conclusion .....</b>	<b>40</b>
<b>8</b>	<b>REFRERENCES.....</b>	<b>41</b>
<b>9</b>	<b>APPENDIX A.....</b>	<b>53</b>
<b>10</b>	<b>APPENDIX B .....</b>	<b>54</b>
<b>11</b>	<b>APPENDIX C .....</b>	<b>55</b>
<b>12</b>	<b>APPENDIX D.....</b>	<b>56</b>
<b>13</b>	<b>APPENDIX E .....</b>	<b>57</b>
<b>14</b>	<b>APPENDIX F .....</b>	<b>58</b>

## **5    ATTRIBUTION**

I would like to thank my co-authors Otto I. Lanz, Noelle M. Muro, Dominique M. Sawyere, Karanvir Aulakh, Theresa Pancotto and David Seda for their contributions and support in the preparation of the manuscript forming a chapter of this dissertation.

Chapter II and the appendices contained within this thesis are previously published in *Frontiers in Veterinary Sciences* under a creative commons copyright. The material has been minimally modified. Dominic C, Lanz OI, Muro N, et al: Titanium-Alloy Anchoring System as a Suitable Method of Extracapsular Repair. *Front Vet Sci* 7:592742, 2020.

## 6 CHAPTER I: LITERATURE REVIEW

### 6.1 Canine Stifle Anatomy

#### 6.1.1 Joint:

The canine stifle is a compound complex condylar synovial joint.<sup>1,2</sup> A compound joint has greater than two articular surfaces enclosed within the same joint capsule.<sup>1</sup> In the stifle, the articular surfaces of the patella and femoral trochlea form the femoropatellar articulation.<sup>1</sup> The femorotibial articulations are formed between the paired medial and lateral femoral and tibial condyles, and are the main weight-bearing articulation of the stifle.<sup>1</sup> The femoropatellar and femorotibial articulations function in concert due to their complex ligamentous attachments.<sup>1</sup> Motion at the femorotibial articulations subsequently induce motion of femoropatellar articulation.<sup>1</sup> A condylar joint is formed between bones with complimentary rounded and depressed condyles.<sup>1</sup> The stifle is considered a complex condylar joint due its rounded femoral and tibial condyles, between which are interposed fibrocartilaginous menisci.<sup>1</sup> Its further classification as a synovial joint is attributed to the ability for motion across the joint.<sup>1</sup> The stifle is capable of motion in multiple planes, but its primary ability to flex and extend, and limited ability to internally and externally rotate further support its classification as a condylar joint.<sup>1</sup>

#### 6.1.2 Bones:

The stifle is composed of three long bones and four sesamoid bones.<sup>1</sup> The long bones which form the canine stifle include the femur, the tibia and the fibula.<sup>1</sup> The distal femur has a quadrangular structure, and its articular surfaces contribute to the femoropatellar and femorotibial joint surfaces.<sup>1,3</sup> The trochlea is the articular surface at the cranial aspect of the femur, which articulates with the patella.<sup>1,3</sup> The trochlea has raised medial and lateral ridges that form a groove in which the patella glides during joint motion.<sup>3</sup> The articular surface of the trochlea is continuous with the articular surfaces of the femoral condyles.<sup>3</sup> These form the femoral components of the femorotibial articulations.<sup>1,3</sup> The medial and lateral femoral condyles are roller-like caudal protrusions of the distal femur that are separated from each other by an intercondylar fossa.<sup>3</sup> Both condyles are convex in the sagittal and frontal planes; however, the medial condyle is smaller and less convex in the sagittal and transverse plane as compared to the lateral condyle.<sup>3</sup> Furthermore, the medial condyle of the femur extends further caudally compared to the lateral condyle.<sup>4</sup> This anatomic difference has potential ramifications on the structures within the medial aspect of the joint as they are consequently exposed to a smaller contact area<sup>3,4</sup> and therefore a higher concentration of pressure when the joint is loaded.<sup>4</sup>

The proximal tibia is triangular in shape, with the apex of the triangle pointed cranially.<sup>3</sup> It has medial and lateral condyles that articulate with the medial and lateral femoral condyles, respectively.<sup>1,3</sup> These condyles form the remaining component of the femorotibial joint.<sup>1,3</sup> The medial condyle is oval in shape, while the lateral condyle is more circular, yet both have a similar total surface area.<sup>3</sup> Each condyle is convex in the sagittal plane and convex in the transverse plane.<sup>3</sup> The tibial condyles are separated from each other by an intercondylar

eminence, with medial and lateral intercondylar tubercles.<sup>3</sup> These tubercles articulate with the femur on their abaxial surface and are non-articular on their axial surfaces.<sup>3</sup> Cranial and caudal to the intercondylar eminence are the cranial and caudal intercondylar areas.<sup>3</sup> The cranial intercondyloid area is oval in shape and is the insertion site for the cranial cruciate ligament and cranial meniscal ligaments.<sup>3</sup> The caudal intercondyloid area is the insertion site for the caudal meniscal ligaments.<sup>3</sup> The tibial tuberosity is the most cranial prominence of the proximal tibia; it is the insertion site of the patellar ligament.<sup>3</sup> Extending distally from the tibial tuberosity is the cranial border of the tibia or tibial crest.<sup>3</sup> This crest serves as a site for muscle attachment.<sup>3</sup> The lateral surface of the proximal tibia has a groove through which the long digital extensor tendon passes, aptly named the extensor groove.<sup>3</sup> On either side of the groove are the cranial and caudal eminences.<sup>3</sup> The caudal border of the proximal tibia has the popliteal notch that separates the medial and lateral tibial condyles<sup>3</sup> and is the insertion site for the caudal cruciate ligament.<sup>1</sup>

The fibula contributes to the stifle joint through its articulation with the tibia.<sup>1</sup> The fibular head has a small tubercle on its medial surface that articulates with the caudolateral portion of the lateral tibial condyle.<sup>3</sup>

The sesamoid bones of the stifle consist of the patella, the paired fabellae, and the popliteal sesamoid.<sup>3</sup> The patella is the largest sesamoid in the body, and is an ossification within the tendon of the quadriceps.<sup>1,3</sup> It is also the origin of the patellar ligament.<sup>1,3</sup> The patella has a proximal base and distal apex.<sup>3</sup> It is oval in shape and convex on its articular surface.<sup>3</sup> Its nutrient foramina enter along its medial aspect.<sup>3</sup> The medial and lateral fabellae are located within their respective heads of the gastrocnemius muscle.<sup>3</sup> The medial fabella is smaller compared to its lateral counterpart and angular in shape.<sup>3</sup> It may articulate with the medial femoral condyle, but this articulation is not always present.<sup>3</sup> The lateral fabella is larger, more globular in shape, and articulates with the lateral femoral condyle.<sup>3</sup> The popliteal sesamoid is located within the origin of the popliteus muscle, and is articular with the caudal aspect of the lateral tibial condyle.<sup>3</sup>

### **6.1.3 Joint Capsule:**

The joint capsule of the stifle is the largest joint capsule in the dog<sup>1</sup>, and has both fibrous and synovial layers.<sup>5,6</sup> The synovial joint capsule forms a sac around the femoropatellar, and medial and lateral femorotibial articulations, all of which intercommunicate.<sup>1,5</sup> The femoropatellar sac is the largest of all three.<sup>1</sup> Both the medial and lateral femorotibial sacs are divided into the femoromeniscal and tibiomeniscal components by the fibrocartilaginous menisci.<sup>1,5,6</sup> The joint capsule extends caudally from the proximal aspect of the femoral condyles to include their articulations with the fabellae.<sup>6</sup> The joint capsule of the lateral femorotibial articulation also surrounds the tibiofibular articulation, passes distally through the extensor groove, and partially surrounds the popliteal tendon.<sup>1,6</sup> Distal to the patella, the infrapatellar fat pad is interposed between the fibrous and synovial layers of the joint capsule.<sup>1,2,5,6</sup>

### **6.1.4 Musculature:**

Several muscles act to accomplish the complex motions of the stifle joint. These muscles are divided into cranial, caudal and medial thigh musculature, the rump muscles, and the muscles of the crus.<sup>6</sup>

The cranial thigh musculature is composed of the quadriceps unit and articularis genus.<sup>6</sup> The quadriceps unit is composed of four individual muscle bellies: the rectus femoris, vastus lateralis, vastus intermedius and vastus medialis.<sup>6,7</sup> Distally, these muscle bellies form the patellar tendon, in which the patella is found.<sup>1,7</sup> This patellar tendon continues as the patellar ligament to insert on the tibial tuberosity.<sup>1</sup> Each muscle belly is innervated by the femoral nerve, and the main function of the quadriceps is extension of the stifle.<sup>6,7</sup> The vastus lateralis, intermedius and medialis originate on the proximal femur.<sup>6,7</sup> The rectus femoris is the sole component to originate via a short, thick tendon from the ilium immediately cranial to the acetabulum.<sup>6,7</sup> As such, it has the added function of flexing the hip.<sup>6,7</sup> The articularis genus is a small muscle that originates proximal to the femoral trochlea on the cranial surface of the femur and inserts on the femoropatellar joint capsule.<sup>6,7</sup> It is innervated by the femoral nerve and functions to flex the stifle.<sup>6,7</sup>

The caudal thigh muscles include the biceps femoris, semitendinosus, semimembranosus, and caudal crural abductor.<sup>6,7</sup> The biceps femoris covers the craniolateral thigh and has two heads.<sup>6,7</sup> The superficial (cranial) head is the larger of the two and originates from the sacrotuberous ligament and ischiatic tuberosity.<sup>6,7</sup> This head blends with the semitendinosus<sup>7</sup> as well as the aponeurosis of the tensor fascia lata.<sup>6,7</sup> As such, it inserts on the patella, patellar ligament and tibial tuberosity; the latter occurs by way of the patellar ligament.<sup>6,7</sup> It is innervated by the sciatic and caudal gluteal nerves and functions to flex the stifle and extend the hip.<sup>6,7</sup> The deep (caudal) head is smaller and originates from the ischiatic tuberosity.<sup>6,7</sup> It inserts on the cranial border of the tibia and the calcaneus as part of the common calcaneal tendon.<sup>6,7</sup> These insertions allow it to flex the stifle and extend the hock, respectively.<sup>6,7</sup> Innervation to the deep head is via the sciatic and tibial nerves.<sup>6,7</sup> The semitendinosus originates between the biceps femoris and semimembranosus on the ventral aspect of the ischiatic tuberosity.<sup>6,7</sup> It inserts on the proximal, medial surface of the tibia as part of the crural fascia.<sup>6,7</sup> It has another insertion as part of the calcaneal tendon.<sup>6,7</sup> It is innervated by the sciatic nerve and functions to flex the stifle and extend the hip and tarsus.<sup>6,7</sup> The semimembranosus originates on the ventral surface of the ischiatic tuberosity medial to the semitendinosus, and has a cranial and caudal belly.<sup>6,7</sup> The cranial belly attaches to the distal medial lip of the femur with the adductor magnus et brevis.<sup>6,7</sup> The caudal belly inserts deep to the medial collateral ligament of the stifle at the level of the medial tibial condyle.<sup>6,7</sup> The cranial belly extends the hip and has no effect on stifle motion.<sup>6,7</sup> The caudal belly will extend the hip and flex the stifle. Both bellies receive nervous supply from the sciatic nerve.<sup>6,7</sup> The caudal crural abductor is a much smaller muscle that originates from sacrotuberous ligament and inserts within the crural fascia.<sup>6,7</sup> It will flex the stifle and abduct the limb.<sup>6,7</sup> It is innervated by the sciatic nerve.<sup>6,7</sup>

The sartorius is a muscle of the medial thigh and has a cranial and caudal belly.<sup>6,7</sup> The cranial belly originates from the iliac crest and ventral iliac spine and inserts with the medial femoral fascia.<sup>6,7</sup> It functions to extend the stifle and flex the hip.<sup>6,7</sup> The caudal belly of the sartorius originates on the tuber coxae and inserts with the crural fascia along the cranial border of the tibia.<sup>6,7</sup> The caudal belly will flex the stifle and hip. Both bellies are innervated by the saphenous

nerve.<sup>6,7</sup> The gracilis, another muscle of the medial thigh, originates on the pelvic symphysis and inserts with the crural fascia on the proximomedial tibia as well as with the semitendinosus as part of the calcaneal tendon.<sup>6,7</sup> It functions to flex the stifle, extend the hip and tarsus, and adduct the limb. It receives its innervation via the obturator nerve.<sup>6,7</sup>

Tensor fascia lata is a triangular muscle of the rump that originates from the tuber coxae, the adjacent portion of the ilium, and from the aponeurosis of the middle gluteal.<sup>6,7</sup> It inserts on the patella via the lateral femoral fascia, and receives nervous supply from the cranial gluteal nerve.<sup>6,7</sup> It extends the stifle and flexes the hip.<sup>6,7</sup>

Muscles of the crus that affect stifle motion include the gastrocnemius, the superficial digital flexor, and the popliteus.<sup>6,7</sup> The gastrocnemius has medial and lateral heads, which originate from the medial and lateral supracondylar tuberosities of the femur, respectively.<sup>6,7</sup> Both heads insert on the calcaneus as part of the calcaneal tendon.<sup>6,7</sup> Through innervation from tibial nerve it serves to flex the stifle and extend the tarsus.<sup>6,7</sup> The superficial digital flexor muscle originates with the lateral head of the gastrocnemius from the lateral supracondylar tuberosity of the femur.<sup>6,7</sup> It inserts distally on the tuber calcanei as part of the common calcaneal tendon and continues to insert on the middle phalanx of digits II-V.<sup>6,7</sup> It is also innervated by the tibial nerve and flexes the stifle.<sup>6,7</sup> Additionally, it extends the hock and flexes digits II-V, which are its major functions.<sup>6,7</sup> The popliteus muscle originates via a tendon from the caudal articular surface of the lateral femoral condyle and inserts on the proximal third of the medial border of the tibia.<sup>6,7</sup> The tendon of origin contains the popliteal sesamoid.<sup>6,7</sup> The popliteus is innervated by the tibial nerve and serves to flex the stifle and cause medial rotation of the crus.<sup>6,7</sup> It may also provide proprioceptive information about the stifle to the central nervous system.<sup>6,7</sup>

### **6.1.5 Vascular Supply:**

Arterial blood supply to the pelvic limb is via the paired external iliac arteries, which are large branches of the abdominal aorta.<sup>8</sup> These arteries originate from the lateral aspect of the aorta ventral to the L6-L7 intervertebral disc.<sup>8</sup> It gives rise to the deep femoral artery and continues as the femoral artery after passing through the abdominal wall.<sup>8</sup> The deep femoral artery is both intra- and extra-abdominal.<sup>8</sup> It originates on the caudomedial aspect of the external iliac artery and exits the abdominal cavity via the vascular lacuna at its caudal aspect.<sup>8</sup> Once outside the abdomen, it becomes the medial circumflex femoral artery.<sup>8</sup> This vessel supplies branches to the iliopsoas, vastus medialis and adductor muscles.<sup>8</sup> It is also the principle nutrient artery of the femur, entering the femur on its caudal surface distal to the greater trochanter.<sup>8</sup>

The femoral artery is the continuation of the external iliac artery after it passes through the vascular lacuna.<sup>8</sup> It is superficial within the femoral triangle, cranial relative to the femoral vein, and covered by the skin and fascia of the proximal, medial thigh.<sup>8</sup> The femoral artery branches extensively within the limb with several of these branches providing arterial supply to the stifle and its associated tissues.<sup>8</sup> These branches include superficial circumflex iliac, lateral circumflex femoral, muscular branches, proximal caudal femoral, saphenous, descending genicular, middle caudal femoral, and distal caudal femoral.<sup>8</sup> As the femoral artery passes along the caudal aspect of the stifle, it changes name to the popliteal artery that also supplies arterial blood to the stifle.<sup>8</sup>

The superficial circumflex iliac is the most proximal of the major branches of the femoral artery.<sup>8</sup> The superficial circumflex iliac originates on the lateral surface of the femoral artery near the lateral circumflex femoral artery, or in some cases it may originate from the lateral circumflex femoral artery itself.<sup>8</sup> Through its course it provides branches into the tensor fascia lata muscle, rectus femoris and the proximal two thirds of the cranial belly of sartorius.<sup>8</sup>

The next branch to come off the femoral artery is the lateral circumflex femoral artery.<sup>8</sup> This artery arises from the caudolateral aspect of the femoral artery and forms many other smaller branches throughout its course: the ascending, transverse and descending branches.<sup>8</sup> It provides branches to supply the iliopsoas muscle, tensor fascia lata and quadriceps.<sup>8</sup> The lateral circumflex femoral artery is the major vessel that supplies the quadriceps muscles.<sup>8</sup>

Distal to the origin of the lateral circumflex femoral artery, the femoral artery provides many variable and inconsistent muscular branches.<sup>8</sup> The proximal caudal femoral artery is the next branch of the femoral artery moving distally along its course.<sup>8</sup> The proximal caudal femoral artery originates from the caudal aspect of the femoral artery and continues along its path distal and caudal crossing the insertion of pectineus, followed by the adductor muscle.<sup>8</sup> The proximal caudal femoral arteries will supply branches to the gracilis, pectineus and adductor muscles along its course.<sup>8</sup> The saphenous artery is a small branch of the femoral artery originating from its medial surface.<sup>8</sup> The saphenous artery provides blood supply to gracilis and caudal belly of sartorius.<sup>8</sup> The saphenous artery passes over the medial surface of the stifle and provides either a single or paired genicular branches that supply the skin and superficial fascia overlying the medial aspect of the joint.<sup>8</sup> The descending genicular artery most commonly arises distal to the origin of the saphenous artery but sometimes may originate with the saphenous as a common trunk off the femoral artery.<sup>8</sup> This vessel is the principle blood supply to the stifle.<sup>5,8</sup> As it passes distally, it courses between the bellies of the vastus medialis and semitendinosus muscles, sending branches to the vastus medialis.<sup>8</sup> At the level of the medial epicondyle it divides into articular branches that supply the medial portions of the femoropatellar and femorotibial joint capsules.<sup>5,8</sup> The middle caudal femoral artery branches from the femoral artery and supplies the adductor and semimembranosus muscles.<sup>8</sup> It will anastomose with the distal caudal femoral artery, which is the next major femoral branch.<sup>8</sup> The distal caudal femoral artery originates on the caudal aspect of the femoral artery.<sup>8</sup> It supplies arterial flow to a number of muscles including the distal biceps femoris, adductor, vastus lateralis, semitendinosus, semimembranosus and gastrocnemius, although supply to some of these muscles is inconsistent and may arise directly from the femoral artery itself.<sup>8</sup>

As the femoral artery passes through the popliteal fossa, it becomes the popliteal artery.<sup>8</sup> The popliteal artery passes between the paired medial and lateral heads of the gastrocnemius muscle.<sup>8</sup> The popliteal artery provides branches to supply the stifle as it passes along its caudal aspect, including middle genicular, medial and lateral proximal and distal genicular arteries.<sup>5,8</sup> These branching vessels supply the greatest amount of blood to the stifle, and they supply the joint capsule, cranial and caudal cruciate ligaments, and medial and lateral collateral ligaments.<sup>5,8</sup> The popliteal artery also branches to provide the sural arteries.<sup>8</sup> These arteries supply the gastrocnemius, popliteal muscle and paired collateral ligaments of the stifle.<sup>8</sup> The popliteal artery also provides a direct branch to supply the tibiofibular joint capsule.<sup>8</sup> As the popliteal artery reaches the interosseous space between the tibia and fibula it divides into the larger cranial tibial

and smaller caudal tibial arteries.<sup>8</sup> The caudal tibial artery will supply blood to lateral digital flexor but is also the nutrient artery of the tibia.<sup>8</sup> The cranial tibial artery supplies the joint capsule of the stifle via branching of the recurrent cranial tibial artery.<sup>8</sup> The cranial tibial artery will also supply the cranial tibial and long digital extensor muscles as well as nutrient arterial supply to the tibia and fibula.<sup>8</sup>

The venous drainage of the pelvic limb can be broadly categorized into superficial and deep veins.<sup>9</sup> The superficial veins of the pelvic limb include the lateral saphenous vein, medial saphenous vein, femoral vein and superficial branch of the deep circumflex iliac vein.<sup>9</sup> The lateral saphenous vein is formed from its cranial and caudal branches and continues to drain into the distal caudal femoral vein.<sup>9</sup> Similarly, the medial saphenous vein is formed from cranial and caudal branches on the medial aspect of the stifle.<sup>9</sup> Following formation of the medial saphenous vein it receives a tributary, the medial genicular vein, which drains the stifle.<sup>9</sup> The superficial branch of the deep circumflex iliac vein receives blood from the skin covering the dorsal two thirds of the abdominal wall in its caudal half.<sup>9</sup> There are several deeper veins of the pelvic limb including the cranial tibial vein, caudal tibial vein, popliteal vein, distal caudal femoral vein, middle caudal femoral vein, superficial circumflex iliac vein, medial and lateral circumflex femoral veins, and several others.<sup>9</sup> The cranial tibial vein receives blood from the cranial crural muscles.<sup>9</sup> It passes through the interosseous space between the tibia and fibula to join the caudal tibial vein forming the popliteal vein.<sup>9</sup> As the popliteal vein moves dorsally passing through the popliteal notch and entering the popliteal fossa, it receives medial and lateral tributaries from the respective aspects of the stifle.<sup>9</sup> More tributaries join the popliteal vein, which changes its name to continue as the femoral vein once it passes the origin of the gastrocnemius.<sup>9</sup> The first tributary to feed into the femoral vein is the distal caudal femoral vein.<sup>9</sup> This vein drains the distal caudal thigh and proximal caudal muscles of the crus, as well as receiving the lateral saphenous vein.<sup>9</sup> The middle caudal femoral vein drains the biceps femoris, gastrocnemius, quadriceps, adductors, semimembranosus and semitendinosus prior to joining the femoral vein.<sup>9</sup> The proximal caudal femoral vein enters the femoral vein and brings blood from the gracilis and adductor muscles.<sup>9</sup> The lateral circumflex femoral vein is the largest and final tributary of the femoral vein.<sup>9</sup> The femoral vein then passes through the vascular lacuna and by doing so becomes the external iliac vein, similar to its arterial counterpart.<sup>9</sup> The deep femoral vein, which receives the medial circumflex femoral vein, also enters the external iliac vein.<sup>9</sup>

### **6.1.6 Lymphatics:**

The lymphatic system of the canine pelvic limb can be sub-divided into three main collecting systems: the superficial lateral system, the superficial medial system and the deep medial system.<sup>10</sup> These systems drain into the popliteal, iliofemoral, and inguinofemoral lymph centers, with extensive and redundant cross-drainage between them.<sup>10</sup> The superficial popliteal lymph node is the sole popliteal lymph node in the canine and the largest lymph node of the pelvic limb.<sup>10</sup> The entirety of the pelvic limb distal to its location will drain to the popliteal lymph center.<sup>10</sup> Efferent lymphatics of the popliteal lymph center will course proximally, and drain into the medial iliac lymph nodes.<sup>10</sup> The iliofemoral lymph center contains the external iliac lymph nodes and distal femoral lymph node, when present.<sup>10</sup> The external iliac lymph node receives lymph from the musculature and bones of the crus and thigh, gluteal musculature, popliteal lymph center and inguinofemoral lymph center.<sup>10</sup> The afferent lymphatics of the iliofemoral

lymph center will drain to the medial iliac lymph nodes, similar to the popliteal lymph center.<sup>10</sup> The distal femoral lymph node will drain the skin over the medial aspect of the pelvic limb, including the pes, crus and stifle.<sup>10</sup> The distal femoral lymph node will also receive afferent lymphatics from the popliteal lymph node.<sup>10</sup> Finally, the inguinofemoral lymph center contains the superficial inguinal lymph nodes.<sup>10</sup> These lymph nodes receive lymph from the medial thigh, stifle, crus and popliteal lymph node, as well as other areas.<sup>10</sup> These lymph nodes also drain to the medial iliac lymph nodes.<sup>10</sup>

### **6.1.7 Innervation:**

Several nerves are important to the function of the pelvic limb and stifle. These nerves are formed from branches of the lumbar and sacral nerves, which include: the femoral nerve, saphenous nerve, obturator nerve, cranial gluteal nerve, sciatic nerve, common fibular nerve and tibial nerve.<sup>11</sup> The ventral branches of the last five lumbar and three sacral nerves form the lumbosacral plexus.<sup>11</sup> Subsequent branching and formation of nerves that innervate the pelvic limb originate at this plexus.<sup>11</sup> The lumbar portion of this plexus will form the nerves that innervate the cranial and medial muscles of the thigh, while the sacral portion will give rise to the nerves that innervate the muscles of the caudal thigh and entire crus and pes.<sup>11</sup> The femoral nerve arises from the lumbar plexus and is formed from ventral branches of lumbar nerves four through six.<sup>11</sup> The femoral nerve provides innervation to all four muscles forming the quadriceps unit.<sup>6,11</sup> The saphenous nerve is a smaller branch off the femoral nerve with both muscular and cutaneous branches.<sup>11</sup> The muscular branch further divides to supply the cranial and caudal bellies of the sartorius muscle.<sup>6,11</sup> The obturator nerve is formed from the ventral branches of the fourth through sixth lumbar nerves, similar to the femoral nerve.<sup>11</sup> After exiting through the obturator foramen, this nerve innervates the gracilis and adductor muscles affecting the stifle, as well as the external obturator and pectineus.<sup>6,11</sup> The lumbosacral plexus contains the lumbosacral trunk, which will eventually continue as the sciatic nerve.<sup>11</sup> Prior to becoming the sciatic, the lumbosacral trunk gives rise to the cranial gluteal nerve.<sup>11</sup> This nerve will supply the cranial and caudal gluteal muscles before terminating in the tensor fascia lata.<sup>11</sup> The lumbosacral trunk becomes the sciatic nerve at the union of the lumbosacral trunk and second sacral nerve.<sup>11</sup> This occurs at the greater ischiatic foramen, and therefore the sciatic nerve constitutes the extra-pelvic portion of the lumbosacral trunk.<sup>11</sup> The sciatic nerve is the largest nerve in the body and provides many muscular branches which innervate the muscles of the caudal thigh including biceps femoris, semitendinosus, semimembranosus and abductor cruris caudalis.<sup>6,11</sup> The sciatic will continue as the smaller common fibular and larger tibial nerves.<sup>11</sup> The common fibular nerve will send an articular branch to supply the lateral collateral ligament of the stifle.<sup>11</sup> The tibial nerve supplies all muscles on the caudal aspect of the crus, therefore it is responsible for innervation to the gastrocnemius, superficial digital flexor and popliteal muscles.<sup>6,11</sup> The tibial nerve also provides branches that innervate the stifle joint.<sup>11</sup>

### **6.1.8 Meniscus:**

Interposed between the femoral and tibial condyles are the medial and lateral menisci of the stifle. The menisci are crescent-shaped discs of fibrocartilage with thin, concave axial and thicker, convex abaxial surfaces.<sup>1,5,6</sup> This structure makes the menisci wedge-shaped in the

frontal plane.<sup>6</sup> The lateral meniscus is both larger and thicker compared to its medial counterpart.<sup>6</sup> Both menisci originate from the fibrous layer of the stifle joint capsule and are covered by synovium.<sup>1</sup> The menisci have several ligaments which connect them to the tibia, femur and each other; however, the medial meniscus maintains an additional attachment to the joint capsule via the coronary ligament.<sup>1</sup>

Histologically the menisci are composed of collagen, proteoglycans and glycosaminoglycans; however, they mostly contain water.<sup>6</sup> The proteoglycans within the meniscus are largely responsible for its high water content and therefore influence functionality of the meniscus.<sup>2</sup> The function of the meniscus is complex and its response to load depends on both its solid and fluid components.<sup>2</sup> Under compressive loads, the solid components of the meniscus demonstrate an elastic response to load, while the fluid component is extruded from the meniscus.<sup>2</sup> The predominant effect of load on the meniscus is influenced by speed of loading, with faster loading resulting in a more elastic response and fluid exudation predominating during slower loading.<sup>2</sup> The collagen fibrils that compose the menisci are organized into three distinct layers that support their function.<sup>2</sup> The outer layer is composed of collagen fibrils in a random orientation.<sup>2</sup> This random orientation provides a low-friction surface on which the femoral condyles can glide.<sup>2</sup> Within the deeper layers collagen fibers have both a radial and circumferential orientation.<sup>2</sup> The inner third of the menisci contains the radially orientated fibers that better resist compression.<sup>2</sup> The outer two-thirds contain the circumferentially orientated fibers suggesting these fibers have a more significant role in tension.<sup>2</sup> Radially orientated fibers are also present throughout the meniscal tissue, although far less frequently.<sup>2</sup> These radially orientated fibers are speculated to have a role in preventing longitudinal splitting of the circumferentially orientated fibers.<sup>2</sup>

Vascular supply to the meniscus is via the medial and lateral genicular arteries.<sup>6,12</sup> The medial and lateral genicular arteries provide arterial blood flow to the stifle joint capsule, which further penetrate the joint capsule to supply the abaxial surface of the menisci.<sup>6,12</sup> The menisci are divided into three zones based on this blood supply. The red-red zone, which is the most peripheral or abaxial zone, the intermediate red-white zone, and the most axial white-white zone.<sup>2</sup> The red-red zone composes only 10-25% of the meniscus.<sup>2,5,6,13</sup> The capillaries supplying the meniscus follow a circumferential pattern similar to the collagen fibers in this region, and give off radially orientated capillaries toward the axial surface.<sup>13</sup> The cranial and caudal poles of each meniscus receive blood supply from vascular synovium, which is continuous with the synovium that covers the cruciate ligaments.<sup>6,13</sup> The remaining portions of the meniscus receive nutrients via diffusion from the synovial fluid.<sup>6</sup>

The meniscus serves numerous functions in the stifle that are supported by its structure. In the non-weight bearing joint, the position of the meniscus between the femur and tibia prevents excessive contact between their articular surfaces.<sup>2</sup> During weight-bearing the menisci are responsible for distributing 40-70% of the load across the joint.<sup>2</sup> They help to deliver the load over a larger area, which reduces stress concentration between areas of the femur and tibia and thus protects the articular cartilage of the stifle.<sup>2</sup> During weight-bearing, the load bore by the meniscus is dissipated radially.<sup>2</sup> This results in elongation of the circumferential meniscal fibers in the outer two-thirds of the meniscus, also known as hoop stress.<sup>2</sup> Hoop stress within the meniscus is what prevents the menisci from radial extrusion.<sup>2</sup> Hoop stress is further transmitted from the menisci to the tibia via their cranial and caudal ligamentous attachments.<sup>2</sup> The overall

shape of the meniscus also supports its function to improve joint congruity.<sup>2</sup> The biconcave structure of the meniscus is reciprocal to the convex femoral and tibial condyles.<sup>2</sup>

### 6.1.9 Ligaments:

There are 11 ligaments that directly contribute to the stifle in the dog.<sup>1</sup> These ligaments can be easily broken down into two categories; the femorotibial ligaments and the meniscal ligaments.

The femorotibial ligaments provide most ligamentous support and include the cranial and caudal cruciate ligaments, and the medial and lateral collateral ligaments.<sup>2</sup> The cruciate ligaments are intracapsular, extra-synovial structures, and are named for their location of insertion on the tibia.<sup>2</sup>

The cranial cruciate ligament originates from the caudomedial aspect of the lateral femoral condyle and caudolateral region of the femoral intercondyloid fossa.<sup>1,2,5,14</sup> It courses distally in a craniomedial direction to insert the cranial intercondyloid area of the tibia.<sup>1,2,5,14</sup> The origin and insertion of the cranial cruciate ligament are variable with regards to descriptions of their shape in the literature. Both have been described as fan-shaped, as well as circular and comma-shaped for their origin and insertion, respectively.<sup>6,14</sup> More recently the origin of the cranial cruciate has been described as arrow-shaped in a population of Beagle dogs.<sup>15</sup> The cranial cruciate ligament itself is formed of two bands, the craniomedial and caudolateral, and the caudolateral band is the larger of the two.<sup>2</sup> Similar to the entire ligament itself, each band of the cranial cruciate ligament is named for its relative insertion on the tibia.<sup>2</sup> The craniomedial band occupies the craniomedial portion of the tibial insertion site, and the caudolateral band occupies the caudolateral portion of the insertion site.<sup>2</sup> Recently, Tanegashima *et al.* identified the presence of a third band. This band was inconsistently observed but originated from the caudal aspect of the caudolateral band and inserted caudal to the caudolateral band.<sup>15</sup> Functionally, the cranial cruciate ligament serves to limit cranial translation and internal of the tibia relative to the femur and to prevent hyperextension of the stifle.<sup>14</sup> Arnoczky and Marshall demonstrated, with isolating sectioning, the individual contribution of the craniomedial and caudolateral bands of the cruciate ligament to its overall function.<sup>14</sup> The craniomedial band of the cranial cruciate ligament was taut in both flexion and extension, whereas the caudolateral band was taut in extension.<sup>14</sup> Thus, when the craniomedial band was transected but the caudolateral remained intact, cranial translation of the tibia was present in flexion but not extension.<sup>14</sup> When the caudolateral band was isolated and transected but the craniomedial remained intact, cranial translation of the tibia was absent in both flexion and extension.<sup>14</sup> The functional anatomy of the canine cruciate was confirmed in a subsequent study by Heffron *et al.*<sup>16</sup> Additionally, the cranial cruciate ligament contains mechanoreceptors and proprioceptors that are important for stifle stability throughout range of motion.<sup>17</sup>

The caudal cruciate ligament, which is the larger of the two, also contains two bands.<sup>2,6</sup> It originates from the lateral surface of the medial femoral condyle and courses distally in a caudal direction to insert on the medial aspect of the popliteal notch within the tibia.<sup>1,2,5,14</sup> Its function is to limit caudal translation of the tibia relative to the femur.<sup>14</sup> Caudal translation of the tibia was most evident when the complete ligament was transected versus just the caudal band and a portion of its cranial band.<sup>14</sup>

Each cruciate ligament has a core of collagen fibrils and fibroblasts.<sup>2</sup> Overlying the core is a layer of loose connective tissue and synovium.<sup>2</sup> This outer layer is absent at the point where the cruciate ligaments twist on one another.<sup>2</sup> Vascular supply to the cruciate ligaments is derived from penetrating branches of the medial and lateral genicular arteries, and the descending genicular artery that supplies their overlying synovium.<sup>14</sup> Blood supply to the caudal cruciate ligament is more robust compared the cranial cruciate ligament due to contact with vascular soft tissues along its caudal border.<sup>6</sup>

The medial and lateral collateral ligaments originate from ovoid areas on the medial and lateral epicondyles of the femur, respectively.<sup>1,2,5,18</sup> As the medial collateral ligament passes distally over the joint, it is fused with the medial joint capsule and is connected to the medial meniscus via the coronary ligament.<sup>2,18</sup> It remains superficial to the tibial insertion of the semitendinosus and a bursa at the level of the medial tibial condyle.<sup>6,18</sup> The medial collateral ligament terminates on the medial surface of the proximal tibia.<sup>1,2,5,18</sup> The medial collateral ligament functions mainly to limit valgus motion of the stifle.<sup>18</sup>

The lateral collateral ligament passes over the stifle joint with only loose connective tissue attaching it to the joint capsule.<sup>6,18</sup> Unlike the medial collateral ligament it has no attachment to the lateral meniscus.<sup>2</sup> The lateral collateral ligament has a smaller component that arises from the region of the lateral femoropatellar ligament.<sup>18</sup> This portion of the ligament forms the caudal border of the lateral collateral ligament and fuses with the main portion over the joint surface before separating to insert separately on the head of the fibularis longis muscle.<sup>18</sup> The lateral collateral ligament principally terminates on the head of the fibula with a few fibers inserting on the tibia.<sup>1,2,5</sup> The lateral collateral ligament serves to prevent varus deviation of the stifle.<sup>18</sup> Increased varus brought on by loss of a functional lateral collateral ligament is exacerbated by the concurrent loss of the cranial cruciate ligament, as these structures complement each other's function, and this is observed throughout range of motion in both flexion and extension.<sup>18</sup>

The menisci are supported by several ligaments. The medial meniscus has both a cranial and a caudal meniscotibial ligament that attach the cranial and caudal poles of the meniscus to the cranial and caudal intercondyloid areas.<sup>1,2</sup> The cranial meniscotibial ligament of the medial meniscus inserts more cranial in the cranial intercondyloid area compared to all other ligaments that attach in this region.<sup>1,2</sup> The caudal meniscotibial ligament of the medial meniscus attaches to the tibia in the caudal intercondyloid area.<sup>1,2</sup> The cranial meniscotibial ligament of the lateral meniscus inserts in the cranial intercondyloid area just caudal to the cranial meniscotibial ligament of the medial meniscus and intermeniscal ligament.<sup>1,2</sup> The caudal meniscotibial ligament of the lateral meniscus inserts in the popliteal notch.<sup>1,2</sup> The intermeniscal ligament attaches the medial and lateral menisci as its name implies.<sup>1</sup> It runs from the caudal aspect of the cranial meniscotibial ligament of the medial meniscus to the cranial aspect of the cranial meniscotibial ligament of the lateral meniscus.<sup>1,2</sup> The medial meniscus maintains an attachment to the medial aspect of the joint capsule via the coronary ligament.<sup>2</sup> The lateral meniscus attaches to the femur via the meniscofemoral ligament.<sup>1</sup> It attaches the caudal axial border of the lateral meniscus to the intercondylar fossa along the medial femoral condyle.<sup>1,2</sup>

The patellar ligament is a continuation of the tendon of the quadriceps that inserts on the tibial tuberosity.<sup>1</sup> Between the patellar ligament and synovial layer of the joint capsule is the

intracapsular fat pad.<sup>1,2,5,6</sup> This fat pad thickens at its distal portion.<sup>1</sup> Immediately proximal to its insertion site, the patellar ligament is separated from the tibial tuberosity by a small synovial bursa.<sup>1</sup> The medial and lateral femoral ligaments function to support the maintenance of the patella within the trochlear groove.<sup>1</sup> The lateral femoropatellar ligament is the larger of the two and it attaches from the lateral surface of the patella to the lateral fabella.<sup>1</sup> The medial femoropatellar ligament is smaller and attaches the medial aspect of the patella to the medial epicondyle of the femur.<sup>1</sup> Both the medial and lateral femoropatellar ligaments blend with the medial and lateral femoral fascia.<sup>1</sup> The medial and lateral parapatellar fibrocartilages are attached to the medial and lateral borders of the patella, respectively, and further help to maintain the patella within the trochlear groove.<sup>1</sup>

In addition to the ligaments present within the stifle, there are two tendons that originate within the stifle.<sup>5</sup> The tendon of origin of the long digital extensor muscle is located in the extensor fossa of the femur.<sup>5</sup> The tendon of origin of the popliteus begins in the popliteal fossa.<sup>5</sup> The popliteal fossa is found immediately caudal to the extensor fossa on the distal aspect of the lateral femoral condyle.<sup>5</sup>

## 6.2 Stifle Kinematics

### 6.2.1 Normal Stifle

*Kinematics is the study of motion of a body without considering the effects of mass or forces acting on that body.* When studying kinematics of the stifle, the kinematics should be evaluated over the entire gait cycle. In the dog, the gait is composed of two phases, the stance phase and the swing phase.<sup>2</sup> These phases correspond to when the foot is in contact with the ground versus when the foot is moving through the air, respectively. A complete gait cycle for any individual limb includes one stance phase, followed by one swing phase. Kinematics of the canine stifle are complex with many anatomic components of the stifle being involved in permitting or restricting movement. The effects of any singular component may change over the course of the complete gait cycle and act in concert with other components.<sup>14,18</sup> The combined anatomic components permit the stifle to flex, extend, adduct, abduct, internally and externally rotate.

As previously mentioned, the principal motion of the stifle is flexion and extension.<sup>1,2</sup> Flexion and extension occur in the sagittal plane with 140° of range of motion across the joint.<sup>19</sup> A more recent study has investigated the maximum mean flexion angle, extension angle and range of motion of the stifle in seven breeds of dogs.<sup>20</sup> In this study, maximum angles and range of motion varied significantly among breeds.<sup>20</sup> Mean maximum flexion angles ranged from 29.3° to 39.1°.<sup>20</sup> Mean maximum extension angles ranged from 151° to 164°.<sup>20</sup> Mean range of motion ranged from 117° to 134°.<sup>20</sup> Variations among breeds in this study were attributed to body weight and muscle mass.<sup>20</sup> In another study that examined Labrador Retrievers, median maximum flexion and extension angles were reported as 41° and 161°, respectively.<sup>21</sup> These differ from those reported in the study by Sabanci *et al.*, but result in a similar range of motion.<sup>20,21</sup> Both studies used a universal plastic goniometer for angle measurement, which was shown to provide goniometric results consistent with those measured on radiographs.<sup>21</sup> Flexion and extension

angles have also been shown to vary with the activity being performed.<sup>22</sup> Kim *et al.* investigated the three-dimensional kinematics of the canine stifle in-vivo using fluoroscopy and computed tomography while sitting, walking, trotting and ascending stairs.<sup>22</sup> The authors observed that during the walk and trot, the swing phase had a large degree of flexion followed by a large degree of extension, while the stance phase had a smaller amount of flexion and extension.<sup>22</sup> The authors made several other notable observations including that increasing internal rotation of the tibia was related to increasing flexion of the stifle, but this correlation varied among activities performed.<sup>22</sup> This coordinated movement of the stifle is known as the “screw-home” mechanism.<sup>22</sup> This finding was confirmed in a later study using a similar methodology but involving biplanar fluoroscopy to quantify the three-dimensional kinematics of the stifle.<sup>23</sup>

Throughout flexion and extension, there is also cranial translation of the tibia relative to the femur.<sup>22</sup> This results from the caudal displacement of the femoral condyles as the stifle flexes throughout the swing phase.<sup>24</sup> The cranial cruciate ligament was identified as the major resistance to cranial translation of the tibia relative to the femur in the normal joint.<sup>14</sup> Additionally, the cruciate ligaments resist internal rotation of the tibia as they twist on each other with increasing flexion through the swing phase.<sup>14</sup>

The medial and lateral collateral ligaments function to limit internal and external rotation of the stifle.<sup>18</sup> During extension of the limb both collateral ligaments are taut and limit internal and external rotation.<sup>18</sup> As the stifle becomes increasingly flexed, the origins of the medial and lateral collateral ligaments move closer together. The cranial component of the medial collateral will remain taut in flexion; however, the caudal component will become more lax.<sup>18</sup> In contrast, the entire lateral collateral ligament becomes lax in flexion during the swing phase.<sup>18</sup> As the lateral becomes more lax, axial rotation of the tibia is permitted due to caudal displacement of the lateral femoral condyle.<sup>18</sup> This is analogous to the “screw-home” mechanism of the human stifle.<sup>25</sup> In addition to the laxity of the lateral collateral ligament, the muscles causing flexion of stifle, chiefly the popliteus, gracilis, semimembranosus and caudal belly of sartorius, also cause internal rotation of the stifle.<sup>22</sup>

Messmer *et al.* demonstrated that the caudal horn of the medial meniscus is subjected to greater pressure compared to the cranial horn as the stifle progresses through the gait cycle.<sup>26</sup> Mean pressure within the caudal horn of the medial meniscus was measured to be 860g during extension and increased to 1896g during flexion, returning to 916g as the stifle became extended.<sup>26</sup> The cranial horn of the medial meniscus was measured as 994g in extension and decreased to 422g during flexion before subsequently increasing back to 848g during progressive extension.<sup>26</sup> Pressure within the caudal horn increased during flexion, whereas it decreased in the cranial horn.<sup>26</sup> This may be attributed to caudal displacement of the femoral condyles as the stifle is flexed.<sup>26</sup>

### **6.2.2 The Cranial Cruciate Ligament Deficient Stifle**

Due to its role preventing cranial tibial translation, internal rotation and hyperextension, loss of the cranial cruciate ligament can be expected to produce changes in the gait cycle. Korvick *et al.* used instrumented spatial linkage and radiophotogrammetry to qualify and quantify changes in gait following transection of the cranial cruciate ligament in five dogs.<sup>27</sup> This involved

application of modified bone plates to the femur and tibia of each dog that would allow consistent placement of the linkage system, and implantation of metallic markers within the femur and tibia to allow radiographic determination of the coordinate system.<sup>27</sup> Additionally, force plate analysis was used to further determine changes in peak vertical force and vertical impulse between conditions.<sup>27</sup> Changes in stifle motion were determined using six degrees of freedom.<sup>27</sup> The authors found that transection of the cranial cruciate ligament resulted in 5-14° more flexion of the stifle at a walk and a 60% decrease in peak vertical force.<sup>27</sup> The authors speculated that this was likely a compensatory response by the dogs to off-load their affected limb; this reduces pain and cranial tibial displacement that occurs when the limb is in an extended position during the stance phase of the gait cycle.<sup>27</sup> The increase in flexion may be due to conscious changes in muscle contraction or as a result of unconscious reflex inhibition of the quadriceps.<sup>27,28</sup> Changes in flexion were less obvious when the dogs were trotting versus walking.<sup>27</sup> Similarly, another study has shown a decrease in peak vertical force following CrCL transection that improved over time but remained decreased two years following surgery.<sup>29</sup> Decreased loading of the affected limb did not result in increased loading of the contralateral limb.<sup>29</sup>

Loss of the cranial cruciate ligament also leads to an increase in cranial translation of the tibia relative to the femur.<sup>27</sup> Cranial tibial thrust was postulated to be secondary to the forces exerted on the stifle by weight-bearing.<sup>30</sup> This theory evolved to include additional factors like muscle contraction and other stabilizers of the stifle including the cranial cruciate ligament and caudal pole of the medial meniscus.<sup>31</sup> In contrast to the theory put forth by Slocum, Tepic *et al.* suggested that the forces generating tibial thrust are parallel to the patellar ligament versus the functional axis of the tibia.<sup>32</sup> In the study by Korvick *et al.*, cranial tibial translation increased from <1mm in the intact limb to roughly 10mm in the transected limb and the greatest amount of translation was noted during the stance phase.<sup>27</sup> In the absence of a functional CrCL, cranial translation of the tibia is limited by the caudal pole of the medial meniscus and thus may predispose the medial meniscus to injury.<sup>33</sup> In the normal stifle the caudal pole of the medial meniscus is subjected to greater pressure during weight-bearing versus the cranial pole; however, this discrepancy is worsened by loss of the CrCL.<sup>26</sup>

Loss of the cranial cruciate ligament also resulted in increased compression across the joint (proximal displacement) and internal rotation of the tibia during the weight bearing stance phase of the gait cycle but resolved during the swing phase.<sup>27</sup> CrCL transection also results in medial displacement of the joint throughout the entire gait cycle.<sup>27</sup> Although transection of the CrCL resulted in changes during the complete gait cycle, most changes were observed and/or more conspicuous during the stance phase leading to the conclusion that this phase of the gait cycle is dependent on a functional CrCL.<sup>27</sup>

Another group of investigators examined the effects of the CrCL-deficient stifle on the gait of dogs over two years.<sup>34</sup> This study further supported the findings by Korvick *et al.* and found a similar degree of cranial tibial translation during the stance phase following loss of the CrCL.<sup>34</sup> Interestingly, over the course of the study period, the tibia was consistently displaced approximately 5mm more cranially at the end of the swing phase, prior to paw-strike.<sup>34</sup> This change occurred mostly during the first year post-transection of the ligament.<sup>34</sup> CrCL-transection also led to increases in medial translation; however, these changes were observed only during the

first year and may have improved with fibrous tissue and/or osteophyte formation over time.<sup>34</sup> Increased abduction following transection of the ligament remained relatively static from the immediate postoperative period and was attributed loss of the CrCL rather than post-liminary meniscal damage or progressive cartilage damage.<sup>34</sup> In contrast to other kinematic and functional analysis studies, loss of the CrCL in this population of dogs did not result in increased internal rotation.<sup>34</sup> On the contrary, these dogs had a mild decrease in the amount of internal rotation observed prompting the authors of this study to question whether internal rotation is limited more by the bones and muscles of the pelvic limb rather than the CrCL.<sup>34</sup>

Kinematic changes to the CrCL-deficient stifle were studied in a population of dogs with naturally occurring CrCL rupture using non-invasive three-dimensional fluoroscopic evaluation.<sup>28</sup> This study found that stifles lacking a functional CrCL maintained the limb in greater flexion throughout the entire gait cycle.<sup>28</sup> The CrCL-intact and CrCL-deficient groups had extension angles of 137-147° and 124-130°, respectively during the stance phase.<sup>28</sup> The CrCL-intact and CrCL-deficient groups had extension angles of 104-146° and 95°-130°, respectively during the swing phase.<sup>28</sup> Cranial translation of the tibia was similar to previous reports<sup>27,34</sup> and was found to be increased at all time points during the gait cycle but most significantly during the stance phase.<sup>28</sup> Cranial tibial translation during the mid-swing phase was 2.1mm and during the mid-stance phase was 9.7mm.<sup>28</sup> Similar to Tashman *et al.*, the amount of internal rotation observed in the CrCL-deficient stifles was not significantly different from the intact group.<sup>28</sup> Despite a lack of significance in the overall magnitude of change, the CrCL-deficient stifles were internally rotated for a significantly longer portion of the swing phase when compared to the CrCL-intact group.<sup>28</sup> The CrCL-deficient stifle also became maximally internally rotated during mid-stance as compared to mid-swing for the intact stifles.<sup>28</sup>

Loss of CrCL function has also been demonstrated to result in decreased stride length.<sup>35</sup> In a group of dogs with naturally occurring CrCL ruptures the stride length of the affected limb was determined to be between 57-96% of that of the intact limb.<sup>35</sup> Angular velocity, paw velocity and stifle range of motion were also significantly different between paired limbs of the CrCL-deficient and CrCL-intact group, although to varying degrees.<sup>35</sup> It was suggested that these variables may prove effective in comparing outcomes for surgical techniques that aimed at improving stability of the CrCL-deficient stifle.<sup>35</sup>

It is important to note that changes in gait as a result of CrCL-rupture are not isolated to the stifle. DeCamp *et al.* identified that in addition to increases in stifle flexion and decreases in stifle angular velocity, the hip and tarsus are hyperextended.<sup>36</sup> This is suspected to be compensation for the increased flexion of the stifle.<sup>36</sup>

## **6.3 Cranial Cruciate Ligament Disease**

### **6.3.1 Etiopathogenesis**

The underlying cause of cranial cruciate ligament rupture in dogs was thoroughly investigated, but the exact pathogenesis of the disease process remains a subject of substantial debate in the

veterinary literature. Due to the complexity of the disease, it is currently thought to be a multifactorial disease process.

### **6.3.1.1 Genetic:**

Several studies have demonstrated an increased propensity for CrCL rupture in certain dog breeds, with large breeds being more commonly affected.<sup>37-41</sup> Breeds including Rottweilers, Newfoundlands, Staffordshire Terriers, Labrador Retrievers, Bulldogs, Boxers, and others have been shown to be at higher risk from suffering a CrCL rupture.<sup>38,39,41,42</sup> In contrast, other studies have demonstrated that Boxers are not at an increased risk.<sup>38</sup> Newfoundlands have received particular attention in genetic studies and a recessive mode of inheritance was identified within this breed.<sup>40</sup> The same study calculated a heritability coefficient of 0.27 within their population study indicating that 27% of cases are owing to genetics within this breed, while the remaining 73% of cases are likely due to environmental causes.<sup>40</sup> A subsequent study in Newfoundlands identified four genetic markers that were associated with CrCL rupture and three of the four markers were confirmed with genotyping.<sup>42</sup> Some breeds have also been identified as having a decreased risk of developing CrCL rupture with Dachshunds frequently making the list.<sup>39,41</sup> Other breeds such as the Old English Sheep Dog, Bassett Hound, Greyhound, German Shepherd and many others have also been identified as having a lower risk of CrCL rupture.<sup>38,39,41</sup>

### **6.3.1.2 Age:**

There are conflicting findings within the literature as to which age group of dogs are more affected by CrCL disease.<sup>37-39,41</sup> Whitehair *et al.* and Witsberger *et al.* found that dogs at a more advanced age were more likely to present for CrCL rupture.<sup>39,41</sup> Witsberger *et al.* identified an increased odds ratio of 1.82 for presenting for CrCL rupture when dogs were between four and seven years of age and an odds ratio of 1.48 for dogs greater than seven years of age.<sup>41</sup> Whitehair *et al.* found the highest prevalence of disease in dogs between seven and ten years of age.<sup>39</sup> Another investigation had a roughly equal distribution in the number of patients presenting at greater than or less than four years of age; however, large breed dogs were the more common in the younger age group, whereas mixed breed and small breed dogs were more common in the older group.<sup>37</sup> Duval *et al.* further supported that larger breed dogs were more likely to present at a younger age.<sup>38</sup> Histologic studies have shown that decreased vascular supply and degenerative changes increase with age, but large breed dogs demonstrate changes earlier than small breed dogs further supporting these findings.<sup>43,44</sup>

### **6.3.1.3 Sex/Neuter Status:**

The incidence of CrCL rupture is higher in female versus male dogs as evidenced by several studies.<sup>37-42,45</sup> This finding is paralleled by well documented evidence of a predilection for human females over males.<sup>46</sup> CrCL rupture is also observed to have a higher incidence in neutered versus intact dogs.<sup>38-42,45</sup> The population that seems to be at greatest risk is therefore spayed females.<sup>38-42,45</sup> In contrast, in one study that segregated affected patients on the basis of age, intact-females were most commonly affected in the less than four years of age group followed by intact males.<sup>37</sup> Intact males were the most commonly affected in the older than four

years of age group followed by intact females.<sup>37</sup> The higher incidence of CrCL rupture in neutered animals may be attributed to increased weight gain following sterilization procedures, but this has not been definitively proven.<sup>39</sup>

#### **6.3.1.4 Body Weight/Obesity:**

Numerous studies have demonstrated that dogs with higher body weights are at increased risk for CrCL rupture.<sup>37-39</sup> A major limitation of many of these studies is the failure to report on body condition scores of the animals. Since many of these same studies report a higher incidence of disease in large breed dogs, there is difficulty in differentiating the effect of increasing body weight due to breed size versus increasing body weight due to obesity. A recent study performed by Santarossa *et al.* compared body weight, body condition scores, muscle condition scores and body composition using dual-energy x-ray absorptiometry as a means to further investigate the relationship between body weight, obesity and presence of CrCL rupture.<sup>47</sup> The investigators found that dogs with CrCL rupture had significantly higher body fat percentage compared to control dogs, 38.78% versus 27.49%, respectively.<sup>47</sup> Affected dogs also had higher body condition scores and lower muscle condition scores compared with unaffected controls.<sup>47</sup> Additionally, two studies have investigated body weight relative to diaphyseal tibial width, termed relative body weight (rBW), as a risk factor for CrCL rupture.<sup>48,49</sup> Both studies concluded that an increase in rBW was associated with the presence of CrCL rupture.<sup>48,49</sup>

#### **6.3.1.5 Conformation:**

Many aspects of the conformation of the pelvic limb have been speculated to play a role in the pathogenesis of CrCL rupture with particular attention given to the tibial plateau angle (TPA).<sup>49-58</sup> The TPA is defined as the acute angle between a line parallel to the tibial plateau and a line drawn perpendicular to the mechanical long axis of the tibia. It was suggested that a steeper tibial plateau subjects the CrCL to increased strain forces and therefore increasing its risk of rupture.<sup>58</sup> As such, many studies have sought to investigate and compare the TPA of various breeds of dogs, and dogs that are affected versus unaffected by CrCL rupture producing conflicting results.<sup>49-51,53-57</sup> Several studies have shown a correlation between increasing TPA and prevalence of CrCL rupture.<sup>49-51,53,55</sup> Wilke *et al.* compared the TPA of a cohort of Greyhounds with those of affected and unaffected Labrador Retrievers.<sup>56</sup> All three groups of dogs within this study had significantly different mean TPAs with affected Labradors have a mean TPA between that of unaffected Greyhounds and unaffected Labradors.<sup>56</sup> This led the authors to conclude that having a steep TPA does not mean all dogs will develop CrCL rupture supporting a multifactorial disease process for this condition.<sup>56</sup> It is worth noting in the literature that affected small breed dogs consistently have higher TPAs compared to affected large breeds. The mean TPA of affected small breeds ranging from 30.1°-32.0° and that of large breeds ranging from 24.9°-28.1°.<sup>49,52,55,56</sup> In addition to the TPA, other conformational factors such as intercondylar notch width have been investigated.<sup>53,55,59</sup>

Kyllar *et al.* investigated the histologic changes present within the cranial cruciate ligament in relation to intercondylar notch width.<sup>53</sup> The authors found that the intercondylar notch was asymmetrical and was more narrow at its cranial extent with progressive widening caudally.<sup>53</sup>

The authors also found that increased degenerative changes within the ligament samples correlated with a more narrow intercondylar notch leading to the conclusion that a narrowed intercondylar notch impinges on the CrCL predisposing it to injury.<sup>53</sup> Good *et al.* found a similar asymmetric appearance to the intercondylar notch in people and a similar finding that people with anterior cruciate ligament injuries had a significantly more narrow intercondylar notch.<sup>59</sup> Contrary to these findings, Mostafa *et al.* did not find a significant difference in notch width when comparing affected and unaffected patients.<sup>55</sup> Relative tibial tuberosity width (rTTW) was investigated in a few studies, but again produced conflicting results.<sup>48,49,52,57</sup> A smaller rTTW is proposed to cause an increase in cranial tibial thrust predisposing the CrCL to injury.<sup>48</sup> In at least two studies a smaller rTTW was associated with the presence of a CrCL rupture.<sup>48,57</sup> Further analysis by Guenego *et al.* cast doubt as to the validity of rTTW as a predictive variable.<sup>48,57</sup> Janovec *et al.* did not find a significant difference in the rTTW of affected and unaffected dogs.<sup>49</sup> In addition to the TPA and rTTW, Guenego *et al.* identified that two other variables were significantly different between affected and unaffected dogs.<sup>57</sup> These included the z-angle, which is the angle between the tibial mechanical axis and a line connecting the cranial extent of the tibial tuberosity to a midpoint between the intercondylar tubercles, and the AMA-angle, which is the angle between the tibial anatomic and mechanical axes.<sup>57</sup> Of the four variables examined in their study, the AMA-angle had the greatest overall sensitivity and specificity for predicting CrCL rupture.<sup>57</sup> An AMA-angle of equal to or greater than 1.87° had a sensitivity and specificity of predicting CrCL rupture of 0.941 and 0.965, respectively.<sup>57</sup> Similar to other factors investigated, AMA-angle gives an impression of the caudal angulation of the tibia, thus a larger AMA-angle increases repetitive strain on the CrCL.<sup>57</sup> Several other conformational variables have been investigated with varying levels of support.<sup>48,49,52,55,57,60</sup>

### 6.3.1.6 Degeneration:

Degeneration of the CrCL is thought to play a major role in predisposing the ligament to rupture and several studies have reported on the histologic changes observed in cases of CrCL disease.<sup>13,43,53,61-68</sup> Ruptured CrCLs demonstrate a complete loss of normal tissue architecture in some areas, with evidence of chondroid metaplasia of fibroblasts that predisposes the ligaments to mechanical failure.<sup>43,53,61,69</sup> Degenerative changes are most striking in the central portion of the ligament, and in one study where degenerated ligaments were tested mechanically, nearly all ligaments ruptured midbody.<sup>69</sup> These changes increase with age and can be found in intact ligaments of older dogs suggesting that degeneration precedes rupture of the CrCL.<sup>66,69,70</sup> This is partially attributed to a decrease in vascular supply to the central core region of the ligament that worsens with age and may be related to twisting of the cruciate ligaments around one another at this site.<sup>43,69</sup>

Kyllar & Cizek 2018 confirmed the presence of degenerative changes within the central region of the ligament and demonstrated that this was also the location where the ligament came into contact with the intercondylar notch.<sup>53</sup> Contact with the intercondylar notch is theorized to increase injury to this area of the ligament that occurs from the cruciate ligaments twisting around one another.<sup>53</sup> Hayashi *et al.* suggested that chondroid transformation of cells within the CrCL is a protective mechanism against tissue hypoxia that results from the poor vascular supply to CrCL and/or repeated microinjury.<sup>70</sup> Their theory was supported by their finding of hypoxia inducible factor-1a within epiligamentous tissue surrounding ruptured CrCL.<sup>70</sup> In a separate

study, the authors demonstrated that repeated microtrauma likely plays a role in CrCL rupture by altering collagen fiber structure and therefore function.<sup>66</sup> Degenerated cruciate ligaments have also shown proliferation of both cellular and vascular components with the presence of mitotic figures, binucleate cells, capillary blood vessels and granulation tissue.<sup>61,69</sup> A higher proportion of apoptotic cells within the core and epiligamentous region of ruptured versus intact CrCLs is documented, suggesting that CrCL rupture may result from apoptosis of cells versus necrosis.<sup>65</sup> The authors postulated that rupture of the CrCL may be due to loss of ligament integrity due to the presence of high number of apoptotic cells; however, this relationship could not be demonstrated conclusively.<sup>65</sup> Comerford *et al.* demonstrated changes within the extracellular matrix (ECM) of ruptured CrCL.<sup>62</sup> These changes include higher quantities of immature collagen crosslinks, higher total and sulfated glycosaminoglycans, higher concentrations of pro-matrix metalloproteinase-2, and lower maximum temperature for collagen denaturation versus intact ligaments.<sup>62</sup> These changes may represent a reparative response of the ruptured CrCL but could also represent changes that preceded ligament rupture.<sup>62</sup>

#### **6.3.1.7 Synovitis:**

Several studies have also demonstrated the presence of inflammation within the synovium of affected stifles and speculated its role in the pathogenesis of CrCL rupture.<sup>61,63,64,67,68,71</sup> Doring *et al.* demonstrated a positive correlation between the presence of stifle lymphoplasmacytic synovitis and CrCL degeneration.<sup>64</sup> The degree of synovitis was also positively correlated with increased age and body weight.<sup>64</sup> In this study, 26.8% of stifles that had evidence of ligament degeneration without concurrent synovitis.<sup>64</sup> It was therefore speculated that synovitis plays a role in CrCL pathology.<sup>64</sup> Doring *et al.* found positive correlations for both pro-inflammatory and anti-inflammatory macrophages within the synovium of stifles with degenerated CrCLs; however, the relationship was most positive for pro-inflammatory macrophages.<sup>64</sup> This finding was further substantiated by Yarnall *et al.*, who demonstrated a similar trend of macrophages toward the pro-inflammatory subtype and suggested that pro-inflammatory macrophages may play a role in the progression of CrCL rupture.<sup>68</sup> Another study demonstrated the presence of cathepsin K and tartrate-resistant acid phosphate cells, which promote collagenolysis within the synovium of affected joints.<sup>71</sup> These authors similarly concluded that synovitis likely plays a role in the progressive degeneration of the CrCL.<sup>71</sup>

#### **6.3.1.8 Inactivity:**

A lack of exercise was shown to cause alterations in the CrCL of rabbits, which had a negative impact on ligament health.<sup>72</sup> It was suggested in at least one study that immobility may play a role in subsequent CrCL rupture, but the role of inactivity in ligament degeneration remains poorly investigated.<sup>37</sup>

#### **6.3.1.9 Trauma:**

Traumatic rupture of the CrCL is a rare occurrence but can occur with overloading of the limb, traumatic hyperextension and/or excessive axial rotation of the tibia.<sup>2</sup>

### 6.3.2 Meniscal Injury

Rupture of the cranial cruciate ligament alters joint kinematics and predisposes individuals to meniscal injury.<sup>73</sup> The medial meniscus is more firmly attached to the tibia as compared to its lateral counterpart, and the medial femoral condyle is also more protrusive and has a smaller contact area with the medial meniscus compared to the lateral femoral condyle making it more prone to injury.<sup>4</sup> As a result, the cranial drawer motion present in the CrCL-deficient joint results in increased shearing forces on the caudal pole of the medial meniscus, with the intact meniscus functioning as a return spring for the CrCL-deficient joint.<sup>34,73</sup> The continual strain placed on the medial meniscus predisposes it to injury.<sup>34</sup> Furthermore, pressures within the caudal horn of the medial meniscus have been measured following CrCL transection and were higher compared to those measured in the caudal horn of the CrCL-intact stifle, as well as the cranial horn regardless if the CrCL was intact or transected.<sup>26</sup>

The incidence of meniscal injury following CrCL rupture is highly variable within the literature and a recent review found a frequency between 0-84%.<sup>74</sup> Several methods of diagnosing a meniscal tear have been reported including radiographs, ultrasound, computed tomographic arthrography (CTA), magnetic resonance imaging arthrography (MRA), arthrotomy and arthroscopy, with or without meniscal probing and stifle distractors.<sup>74-82</sup> Arthroscopy with the use of a meniscal probe has repeatedly been shown to be more sensitive in identifying meniscal pathology.<sup>74,78,79</sup>

Few studies specifically examine the risk factors relating to meniscal injury in the CrCL-deficient joint.<sup>83-85</sup> In a 2002 study, factors shown to increase risk of meniscal injury included increasing body weight, collapse of the medial joint space on radiographs, and increasing grades of lameness, joint effusion and osteoarthritis.<sup>85</sup> The same study did not find a significant relationship between duration of lameness or complete CrCL tears and increased risk of meniscal injury.<sup>85</sup> A later study also found that increasing body weight increased the risk of meniscal injury.<sup>84</sup> However, in contradiction to the previous study, these authors found that chronicity of lameness and presence of complete CrCL rupture were significant risk factors for meniscal injury.<sup>84</sup> The risk of meniscal injury increased 12.9 times in the presence of a complete CrCL tear.<sup>84</sup> Additionally, certain breeds including the Rottweiler and Golden Retriever were found to have an increased risk of meniscal injury.<sup>84</sup> A study investigating the relationship between the TPA and risk for meniscal injury found no relationship in the four breeds examined in that study.<sup>83</sup> Meniscal injury plays an important role in the pathogenesis of CrCL disease as it plays a role in the progression of osteoarthritis.<sup>86-88</sup>

### 6.3.3 Osteoarthritis:

Instability of the stifle due to cranial cruciate ligament injury will result in osteoarthritis, and transection of the CrCL is an experimental model for producing osteoarthritis.<sup>89-91</sup> Instability of stifle joint due to loss of the CrCL causes alterations in proteoglycan and glycosaminoglycan content, which results in weaker bonds between collagen fibers.<sup>90</sup> These changes in proteoglycan and glycosaminoglycan content also result in decreased aggregation of proteoglycans and increased water content and swelling of cartilage tissues.<sup>90,92</sup> As a result of the increased water

content, the cartilage surfaces of affected joints appear thicker, and these changes are evident prior to gross fibrillation of the cartilage surface.<sup>90</sup> Gross pathologic changes of fibrillation and ulceration are most severe in the central portion of the medial femoral condyle.<sup>90,92</sup> The absence of meniscal tissue covering this portion of the articular surface may result in greater load-bearing over this portion of the joint surface, predisposing it to more severe degenerative changes.<sup>90</sup> Other changes include thickening of the subchondral bone, osteophyte formation, thickening of the joint capsule and synovitis characterized by mononuclear cell infiltrates.<sup>92</sup>

### **6.3.4 Diagnosis:**

#### **6.3.4.1 Signalment:**

The signalment of patients presenting for CrCL rupture can be varied, but most commonly it affects an older population of dogs between 6.8-10 years of age.<sup>37,39</sup> This is in contrast to certain reports, which demonstrate that a subset of the population may be affected at a younger age, often less than 2 years old.<sup>38</sup> This difference in age for presentation of disease is attributed to breed, with large breeds often presenting at younger ages.<sup>37,38</sup> Several breeds of dogs have repeatedly demonstrated genetic or breed-predisposition for CrCL rupture. These include the Rottweiler, Newfoundland, Labrador Retriever, Neapolitan Mastiff, Saint Bernard, American Staffordshire Terrier, as well as others.<sup>37-40,42,93</sup> Other breeds, such as the German Shepherd or mixed breed dogs, have demonstrated a decreased risk.<sup>38</sup> A discrepancy exists within the literature with certain studies reporting a higher prevalence within the female sex, while other studies demonstrated an equal sex distribution.<sup>37-39,93</sup> Several studies have demonstrated a higher prevalence of disease within neutered animals.<sup>38,39,41,45</sup>

#### **6.3.4.2 History:**

Bennet *et al.* described a roughly equal proportions of acute versus gradual onset of pelvic limb lameness in patients presenting for CrCL-rupture, but in both groups the incidence of witnessed trauma at the time of initial injury was very low.<sup>37</sup> A low incidence of known trauma was also reported by Gambardella *et al.*<sup>94</sup> Patients presenting with acute onset of lameness variably improved, worsened or remained static with respect to their degree of lameness by the time of presentation.<sup>37</sup> In cases of gradual onset lameness, the affected dogs are often described as more lame following periods of inactivity or periods of exercise.<sup>2,37</sup> The lameness was also described as painful in the back end, increased weight bearing on the forelimbs and an unsteady gait.<sup>37</sup> Moreover, the severity of the lameness observed is often related to the degree of instability present, and the lameness resulting from a partial tear may be less severe than that of a complete rupture.<sup>2</sup>

#### **6.3.4.3 Gait Analysis:**

Rupture of the CrCL results in a predictable lameness in affected dogs that was characterized in several studies examining both natural and experimental CrCL disease.<sup>27,35,36</sup> The affected stifle

is more flexed throughout the gait cycle, while the hip and tarsal joints are more extended.<sup>27,28,36</sup> The CrCL-deficient stifle will have a shortened stride compared to a CrCL-intact stifle.<sup>35,36</sup>

#### **6.3.4.4 General palpation:**

General palpation of the CrCL-deficient limb can identify several abnormalities. In cases of chronic CrCL rupture, palpation of the affected limb can reveal atrophy of the quadriceps unit.<sup>95</sup> Additionally, chronicity can lead a thickening of the soft-tissues surrounding the stifle known as medial buttress.<sup>37,95</sup> Effusion that develops within the affected stifle results in a less discernable patellar ligament.<sup>95</sup> Stifle range of motion may reveal crepitus associated with the onset of osteoarthritis.<sup>95</sup>

#### **6.3.4.5 Cranial Drawer:**

Rupture of the CrCL ligament results in instability of the stifle that can be demonstrated by performing a cranial drawer test. Instability is variably present based on the portion of the CrCL that is ruptured.<sup>96</sup> Complete tearing of the CrCL will result in a positive drawer sign throughout range of motion.<sup>96</sup> Partial rupture of the craniomedial band will result in cranial translation of the tibia during flexion but not extension.<sup>96</sup> This is because the intact caudolateral portion of the CrCL remains taught during extension of the stifle and subsequently resists cranial translation of the tibia relative to the femur.<sup>96</sup> Rupture of only the caudolateral band will not result in appreciable instability because the craniomedial band will remain taught during flexion and extension.<sup>96</sup>

#### **6.3.4.6 Cranial Tibial Thrust:**

Cranial tibial thrust is an internal force generated between the femoral condyles and tibial plateau that is neutralized in part by the CrCL.<sup>97</sup> When the cranial cruciate ligament is ruptured, the tibia translates cranially relative to the femur.<sup>97</sup> This is demonstrated by a positive tibial compression test.<sup>98</sup> Assessment of tibial thrust involves resting the index finger on the cranial horn of the medial meniscus and stabilizing the femur.<sup>98</sup> The opposite hand grasps the plantar surface of the metatarsal region and short, upward thrusts to simulate weight-bearing at a standing angle are performed.<sup>98</sup> A positive test results in cranial translation of the tibia relative to the femur.<sup>98</sup> A modified tibial compression test was described by Valen *et al.* where the traditional tibial compression test is performed continuously throughout range of motion during flexion and extension, which may better aid detection of medial meniscal injuries.<sup>99</sup>

#### **6.3.4.7 Meniscal Click:**

A meniscal click is the audible or palpable click that can sometimes be appreciated during examination of the CrCL-deficient stifle due to displacement of a damaged medial meniscus.<sup>100</sup> This test is characterized by a low sensitivity ranging from 31-45.8% and high specificity ranging from 94.4-96% in the awake patient.<sup>101-103</sup> When a meniscal click and pain on stifle flexion were present concurrently, the sensitivity for detection of a meniscal tear was increased

to 85%, while specificity decreased to 57%.<sup>101</sup> Accuracy of a meniscal click for detecting meniscal injury is reported between 63-75%.<sup>101-103</sup> The majority of patients with a palpable meniscal click and confirmed meniscal injury had a bucket handle tear of the medial meniscus.<sup>102,103</sup> Presence of a meniscal click was significantly associated with the presence of bucket-handle tears and not significantly associated with non-bucket-handle tears of the medial meniscus in one study.<sup>103</sup>

#### **6.3.4.8 Radiographs:**

Orthogonal lateral and craniocaudal radiographs of the CrCL-deficient stifles often demonstrate pathology supportive of CrCL ligament instability.<sup>95</sup> Effusion develops within the stifle following acute injury of the CrCL and results in cranial displacement of the infrapatellar fat pad.<sup>95</sup> With chronicity, osteophyte and enthesophyte formation become evident, and this is repeatedly documented in several studies of both experimental and naturally occurring cruciate rupture.<sup>37,91,92,95,104,105</sup> Osteophyte formation occurs along the medial and lateral femoral trochlear ridges, medial and lateral tibial condyles, and base and apex of the patella.<sup>37,91,95</sup> Osteophytes at these locations were confirmed on gross inspection of the stifle in an experimental model of CrCL disease.<sup>92</sup> In addition to joint effusion and osteophytosis, cranial displacement of the tibia relative to the femur can be seen.<sup>95</sup> A supplementary finding supportive of CrCL injury is the distal displacement of the popliteal sesamoid bone.<sup>106</sup> Distal displacement of the popliteal sesamoid bone was demonstrated to be 99% accurate and 100% specific of CrCL rupture in a single study.<sup>106</sup> Radiographs can also be used to predict the presence of a medial meniscal tear in dogs with CrCL rupture on a standard 90° lateral radiograph of the stifle.<sup>81</sup> Won *et al.* found that a medial meniscal tear could be predicted in dogs weighing a mean of 31kg with a joint space width of 3.43mm.<sup>81</sup> The sensitivity and specificity of predicting a meniscal tear using this method were 40.5% and 89.5%, respectively.<sup>81</sup>

#### **6.3.4.9 Ultrasound:**

Ultrasound can be used to diagnose CrCL rupture, although making the diagnosis can be difficult. One study reported the ability to diagnosis CrCL rupture by ultrasound in only 15.4% of cases.<sup>75</sup> Ultrasound can however be used to identify secondary abnormalities that occur as a result of CrCL instability such as joint effusion and osteophytosis.<sup>75</sup> In addition, meniscal injury can often be seen on ultrasound with a sensitivity and specificity for detection of meniscal pathology ranging from 82-95% and 78-93%, respectively.<sup>75,107</sup>

#### **6.3.4.10 Computed tomography (CT):**

In an experimental model using cadaver limbs, plain CT was suitable for evaluating the bones comprising the stifle joint; however, intra-articular structures were not visible.<sup>108</sup> The addition of 1.5mL intra-articular sodium and meglumine amidotrizoate, diluted to 185mg I/mL, allowed visualization of the intra-articular structures, and a transected CrCL could be identified in all specimens.<sup>108</sup> Moreover, contrast arthrography had a sensitivity of 90% and specificity of 100% for detecting tears within the caudal pole of the medial meniscus.<sup>108</sup> In a separate study examining clinical patients, CTA was 100% sensitive and 100% specific for diagnosing tears of

the CrCL<sup>80</sup>. The sensitivity and specificity of CTA for diagnosing meniscal injuries was 64.3% and 73.3%, respectively.<sup>80</sup>

#### **6.3.4.11 Magnetic Resonance Imaging (MRI):**

Both MRI and magnetic resonance arthrography (MRA) can be used to identify the structures forming the stifle joint, as well as intra-articular structures like the cruciate ligaments and menisci.<sup>109</sup> MRI can also reveal several abnormalities resulting from CrCL instability, including defects in articular cartilage, increased meniscal signal, loose intra-articular bodies, synovitis and osteophytosis.<sup>91</sup> In a study by Galindo-Zamora *et al.* MRI correctly identified all cruciate ligaments as being ruptured.<sup>77</sup> A separate study by Fazio *et al.* found MRI to have a sensitivity, specificity and accuracy of 78%, 50-60% and 68-71%, respectively for diagnosis of complete CrCL rupture.<sup>76</sup> In the same study, MRI had a sensitivity and specificity of 94.4% and 100% for detected medial meniscal injuries.<sup>77</sup> A recent study found that stress MRI, in which the stifle is placed in drawer or tibial compression, can be used to measure displacement of the tibia relative to the femur.<sup>110</sup>

#### **6.3.4.12 Arthrotomy/Arthroscopy:**

Both arthrotomy and arthroscopy can be used to confirm the presence of a CrCL tear. Arthroscopy is associated with increased cost and requires greater technical skill.<sup>95</sup> Arthroscopy also demonstrates higher sensitivity for detection of meniscal injuries compared to arthrotomy in multiple studies.<sup>74,78,79</sup> It was demonstrated that with either technique, probing of the meniscus will increase the sensitivity for detection of meniscal tears.<sup>79</sup>

### **6.3.5 Treatment Options**

#### **6.3.5.1 Medical Management:**

There are relatively few reports of outcomes of non-surgical management of CrCL rupture in veterinary medicine.<sup>111-113</sup> Non-surgical management often involves a combination of exercise modification, maintenance of a lean body weight, administration of medications such as non-steroidal anti-inflammatories, and rehabilitation.<sup>112,114</sup> In a single study, 83% of patients weighing less than 15kg demonstrated improvement in lameness with medical management versus only 13% of dogs weighing greater than 15kg showed signs of improved lameness without surgery.<sup>112</sup> A separate study evaluating outcomes for overweight patients managed medically alone versus in combination of surgery yielded somewhat contradictory results.<sup>113</sup> In this study nearly two thirds of the medical management group showed improvement and successful outcome by the 52-week recheck.<sup>113</sup> Although these dogs improved, dogs that received surgery in combination with medical management were more likely to have a successful outcome and demonstrated higher peak vertical force of the affected limb at the 24-week and 52-week rechecks.<sup>113</sup> Investigation of a single injection of platelet-rich plasma (PRP) on the progression of stable partial CrCL tears concluded that PRP was ineffective in preventing disease progression.<sup>111</sup> Affected stifles demonstrated increased joint effusion, increased fiber tearing and

decreased ligament volume during the 12 month follow-up period, and 29.6% of dogs developed complete rupture of the ligament.<sup>111</sup> However, in a separate study a single injection of PRP in combination with bone marrow concentrate or adipose-derived progenitor cells demonstrated complete repair and normal fiber alignment in 9/13 dogs when used to treat partial CrCL tears.<sup>115</sup> Despite reported inferior outcomes, conservative management of CrCL rupture for dogs weighing less than 15kg is still commonly recommended by small animal veterinarians.<sup>114</sup>

Numerous methods of surgical intervention are described for the treatment of the CrCL-deficient stifle, and these can be broadly categorized into intracapsular, extracapsular and osteotomy procedures.<sup>116,117</sup> Extensive research exists comparing the various techniques, complication rates and outcomes, but substantial evidence to recommend a single, best procedure does not exist.<sup>116,117</sup> As such, surveys of veterinarians consistently reveal that a variety of procedures are commonly performed to treat CrCL rupture.<sup>118-120</sup> Despite the absence of evidence to support one procedure over all others, considerable research exists comparing extracapsular and osteotomy techniques.<sup>121-127</sup> Some studies report superior owner satisfaction and objective outcomes for osteotomy procedures, mainly tibial plateau leveling osteotomy (TPLO).<sup>124-126</sup> This is balanced by other studies demonstrating similar objective and clinical outcomes between extracapsular methods and osteotomy procedures.<sup>121-123,127</sup>

### **6.3.5.2 Intracapsular Techniques:**

#### **6.3.5.2.1 Paatsama Technique:**

This intracapsular method of repair involves development of a 1-2cm wide fascial strip from the fascia lata of the lateral thigh.<sup>128</sup> The fascial strip is left attached at its distal aspect and pulled through bone tunnels created in the femur and tibia at the origin and insertion of the CrCL, respectively.<sup>128</sup> The fascial strip is secured in the location of the CrCL using orthopedic wire and subsequent suturing to the patellar ligament.<sup>128</sup> Surveys of veterinarians offering surgery for CrCL disease suggest this technique is no longer commonly performed.<sup>114,120</sup>

#### **6.3.5.2.2 Over-the-Top:**

The Over-the-Top technique requires harvesting the medial third of the patellar ligament, a portion of the patella and the patellar tendon.<sup>129,130</sup> The patellar ligament remains attached at its insertion on the tibial tuberosity and the autograft tissue is pulled through the joint to exit through the femorofabellar ligament.<sup>129,130</sup> It is sutured to the lateral femoral condyle in order to mimic the CrCL.<sup>129,130</sup> This technique avoids the creation of bone tunnels that are required in the Paatsama technique.

#### **6.3.5.2.3 Under-and-Over:**

The Under-and-Over procedure creates a similar fascial strip to the original Paatsama technique, but the strip is created distally to the level of the tibia and involves the lateral third of the patellar ligament.<sup>131</sup> The strip is passed under the intermeniscal ligament and pulled through the joint.<sup>131</sup>

The fascial strip is pulled out the caudal aspect of the joint, wrapped around and secured to the femoral condyle using a bone screw and spiked washer.<sup>131</sup> This technique was subsequently modified to avoid the use of the screw and washer, using suture to secure the graft to the lateral femoral condyle.<sup>132</sup>

#### **6.3.5.2.4 Hamstring Graft:**

This autograft technique harvests the crural fascia with the combined insertions of the gracilis and semitendinosus muscles.<sup>133</sup> The insertion of each tendon to the tibia is maintained, while the muscular portions are isolated and transected.<sup>133</sup> The bony insertions are elevated with a strip of crural fascia overlying the medial tibia to just proximal to the talocrural joint.<sup>133</sup> The fascial strip is then twisted on itself and passed proximally into the stifle through a bone tunnel created in the tibia.<sup>133</sup> The graft is passed through the stifle to exit the caudal joint where it is secured over the lateral femoral condyle with bone staples.<sup>133</sup> Long-term follow-up of patients 52 weeks post-CrCL reconstruction showed marked improvements in peak vertical force and vertical impulse, 98% and 90% of the control limbs, respectively.<sup>133</sup>

#### **6.3.5.2.5 Synthetic Graft:**

Barnhart *et al.* reported the use of a synthetic ligament that was a ultra-high molecular weight polyethylene (UHMWPE) core with a braided, porous, non-expanded polytetrafluoroethylene (PTFE) sheath.<sup>134</sup> This ligament is passed through bone tunnels created in the origin and insertion of the CrCL, and exited level with the lateral fabella and proximomedial tibia, respectively.<sup>134</sup> The synthetic ligament was secured to the femur and tibia using bone screws and spiked washers placed perpendicular to the long-axis of the bones.<sup>134</sup> This technique resulted in 32% of patients experiencing at least one major complication and synthetic ligament fixation failure was documented as the most common of the major complications that occurred.<sup>134</sup> This was suspected to be due to poor tissue ingrowth, poor osseous integration of implants and/or failure of the materials.<sup>134</sup> A follow-up study in canine cadavers examining methods of synthetic ligament fixation found that use of a larger interference screw and spiked washer provided the highest strength of fixation in both the femur and tibia compared to using smaller diameter screws without a spiked washer.<sup>135</sup> However, when examining the femur specifically, a 5mm interference screw without the use of a spiked washer provided an ultimate load and stiffness that most closely resembled that of the natural CrCL.<sup>135</sup> The clinical impact of these findings is uncertain.

### **6.3.5.3 Extracapsular Techniques:**

#### **6.3.5.3.1 Lateral Imbrication:**

Childers described lateral imbrication of the joint capsule as a method of extracapsular stabilization of the CrCL-deficient stifle.<sup>136</sup> This procedure involves making an lateral incision through the skin and subcutaneous tissues centered over the stifle.<sup>136</sup> With the leg held in extension, a row of Lembert sutures are placed in the lateral joint capsule causing imbrication of

the fascial tissues.<sup>136</sup> If there was persistent instability following suture placement, a second row of Lembert sutures are placed overlying the first row for additional imbrication.<sup>136</sup> Addition of an overlying second row Lembert sutures regardless of the presence of persistent instability was later described by Pearson.<sup>137</sup> The original technique by Childers was performed in 10 dogs with induced or natural CrCL rupture, and all dogs were reported to be improved postoperatively.<sup>136</sup> Three dogs were followed for six months following surgery and were determined to be free of clinical signs at last follow-up.<sup>136</sup>

#### **6.3.5.3.2 Lateral Retinacular Imbrication:**

In this method the CrCL-deficient stifle is stabilized by placement of a mattress suture within the lateral retinaculum.<sup>138</sup> The suture is passed from immediately caudal and proximal to the lateral fabella, directed craniodistally through the soft tissues to exit the lateral third of the patellar ligament immediately proximal to its insertion site.<sup>138</sup> The needle was then reinserted 3mm from its exit site through the patellar ligament in a proximal and caudal direction to exit near the original insertion site, and the suture is tied.<sup>138</sup> A second suture is placed adjacent to the first. This procedure was reported to be successful 85.7% of dogs.<sup>138</sup>

#### **6.3.5.3.3 Modified Retinacular Imbrication:**

Flo described a modification of the previously reported lateral retinacular imbrication whereby mattress sutures are placed around each of the medial and lateral fabella and anchored to the tibia via a bone tunnel created in the tibial tuberosity.<sup>139</sup> In this technique a third suture is anchored around the lateral fabella and directed to exit at the lateral aspect of the patella.<sup>139</sup> This suture will serve as an imbrication suture.<sup>139</sup> Proposed advantages of this technique over previous imbrication techniques include more robust anchorage of the suture material around the fabellae and tibial tuberosity, protection of the lateral imbrication suture by the addition of a medial suture, and reduced risk of damage to regional neurovascular structures.<sup>139</sup> In the original description, this procedure was successful in 92.5% of cases.<sup>139</sup>

#### **6.3.5.3.4 Lateral Suture:**

This technique involved the placement of three mattress sutures.<sup>94</sup> The first suture was placed around the lateral fabella and through the patellar ligament distal to the patella.<sup>94</sup> The second suture was placed around the lateral collateral ligament, distal to the fabella, and through the patella ligament.<sup>94</sup> The final suture was placed around the lateral collateral ligament distal to the first suture but proximal to the fibular head and also passed through the patellar ligament.<sup>94</sup> All three sutures were preplaced, then tied.<sup>94</sup> At physical follow-up, 94.1% of dogs had no discernable lameness and the remaining dogs were mildly lame during certain activities.<sup>94</sup> Owners determined their dog had normal use of their limb in 97.9% of cases.<sup>94</sup>

#### **6.3.5.3.5 Three-in-One:**

The Three-in-one procedure involves the placement of three circumfabellar sutures.<sup>140</sup> A single circumfabellar suture is placed around the medial fabella and passed through a bone tunnel created in the tibial tuberosity.<sup>140</sup> Two circumfabellar sutures are placed around the lateral fabella.<sup>140</sup> One is passed through the bone tunnel within the tibial tuberosity, while the second is placed through the lateral third of the patellar ligament near its distal attachment.<sup>140</sup> During closure, the lateral fascia is secured to the patellar ligament to tighten the fascial tissues on the lateral aspect.<sup>140</sup> On the medial side, the caudal belly of the sartorius is advanced and sutured to the patellar ligament.<sup>140</sup>

#### **6.3.5.3.6 Fibular Head Transposition:**

With fibular head transposition, a lateral approach to the stifle is performed and retraction of the lateral retinaculum allows identification of the fibular head and lateral collateral ligament.<sup>141</sup> The musculature covering the cranio-lateral surface of the tibia is elevated and an incision is made into the fascia cranial to the lateral collateral ligament.<sup>141</sup> The fibular head and tibia are separated at their articulation.<sup>141</sup> Two holes are drilled through the tibial crest cranial to the fibular head and underneath the lateral tibial musculature.<sup>141</sup> The fibular head is transposed cranially and affixed to the lateral surface of the tibia using a Kirschner wire and figure-of-eight orthopedic wire passed through the previously made bone tunnels in the tibia.<sup>141</sup> Postoperative evaluation of patients receiving fibular head transposition found good to excellent outcomes in 90% of cases.<sup>141</sup>

#### **6.3.5.3.7 Popliteal Tendon Transposition:**

In this technique, a lateral approach to the stifle is performed and the tendon of the popliteal muscle is identified and isolated.<sup>142</sup> The tendon is transected distal to the sesamoid and further freed from the surrounding fascia and joint capsule to its origin on the femoral condyle.<sup>142</sup> The cranio-lateral aspect of the tibia is exposed and a bone tunnel is created with over drilling of the lateral aspect to allow seating of the popliteal sesamoid.<sup>142</sup> A suture is placed through the popliteal tendon proximal to the sesamoid using a Krackow pattern.<sup>142</sup> The tendon is then pulled through the bone tunnel in a lateral to medial direction until the popliteal sesamoid sits within the bone tunnel.<sup>142</sup> The tendon is sutured to the medial aspect of the tibia with a button and tightened until cranial drawer is absent.<sup>142</sup> This technique was performed in five dogs and resulted in significantly decreased internal rotation immediately postoperative.<sup>142</sup> By six months postoperatively no dogs were clinically lame.<sup>142</sup> Following popliteal tendon transposition, the popliteal tendon more closely mimics the orientation of the CrCL than the lateral collateral following fibular head transposition.<sup>142</sup> This technique also better preserves the natural internal rotation of the tibia during stifle flexion, which is lost with fibular head transposition.<sup>142</sup>

#### **6.3.5.3.8 Tightrope:**

The Tightrope technique is an extracapsular method of repair developed by Arthrex that uses Fibertape to stabilize the CrCL deficient stifle.<sup>123</sup> Briefly, bone tunnels are created within the femur and tibia and a continuous strand of Fibertape is passed through both tunnels spanning the stifle joint along its lateral aspect.<sup>123</sup> The Fibertape is tied over buttons covering the medial

aspect of each bone tunnel.<sup>123</sup> Mechanical testing of the Tightrope showed superior stiffness, higher load to yield and lower cycle displacement compared to other extracapsular methods of repair.<sup>123</sup> When performed in clinical patients, the Tightrope procedure had similar subjective outcomes to the tibial plateau leveling osteotomy at six-month postoperative evaluations.<sup>123</sup> Despite a similar complication rate to that of TPLO, a survey of veterinarians revealed a low preference for performing the Tightrope procedure.<sup>120,123</sup> This is due to the perceived risk of prosthetic-associated infection.<sup>120</sup>

### **6.3.5.3.9 Lateral Extracapsular Suture System (LESS):**

This method of stifle stabilization involved placement of two laterally placed titanium-alloy bone anchors, one in the femur and the one in the tibia.<sup>143</sup> The bone anchors are connected by a suture of UHMWPE fiber and PTFE.<sup>143</sup> Proposed advantages of this procedure over a traditional lateral suture technique included osseous points of suture fixation, improved isometry and improved joint range of motion.<sup>143</sup> Biomechanical testing of this procedure demonstrated that internal rotation was not significantly different from a CrCL-intact stifle; however, cranial tibial translation remained significantly increased in the LESS versus CrCL-intact stifle except at a stifle angle of 125°.<sup>143</sup> Clinical reports of this technique are lacking.

### **6.3.5.3.10 Ruby Joint Stabilization System:**

The Ruby system is a modification of the LESS procedure with similar advantages over the traditional lateral suture technique.<sup>144</sup> It involves placement of two titanium-alloy bone anchors within the lateral aspects of the femur and tibia at points demonstrated to approach physiologic isometry with the CrCL.<sup>144</sup> The bone anchors have attached loops of UHMWPE fibers that are connected by a titanium link.<sup>144</sup> The link is then closed and the UHMWPE loops secured by placement of a polyetheretherketone (PEEK) link lock.<sup>144</sup> This procedure was performed clinically in 17 dogs, all of whom had improved lameness scores postoperatively and an early return to weight bearing.<sup>144</sup>

## **6.3.5.4 Osteotomy Procedures:**

### **6.3.5.4.1 Cranial Tibial Closing Wedge Osteotomy (CWCO):**

This osteotomy procedure involves removing a cranially based wedge from the proximal tibia in order to reduce the TPA and neutralize tibial thrust.<sup>145</sup> The osteotomy is stabilized with a medially applied bone plate.<sup>145</sup> In an early report of dogs undergoing CWCO, both short- and long-term follow-up yielded good results, and at 12-months postoperatively there was subjectively no difference between the affected and contralateral normal limb.<sup>145</sup> A more recent report of a modified CWCO also described no difference in short- or long-term lameness score, complication rates, reoperation rates, and owner assessed outcome when compared to the TPLO.<sup>146</sup>

#### **6.3.5.4.2 Tibial Plateau Leveling Osteotomy (TPLO):**

A TPLO is among the most common procedures performed for CrCL rupture.<sup>118,120</sup> This is a geometry-modifying procedure that serves to neutralize tibial thrust by altering the TPA.<sup>31</sup> A radial saw blade is used to make a cut in the caudoproximal portion of the tibia so that the entire tibial condyle can be rotated caudally, thus leveling the tibial plateau.<sup>31</sup> A medially applied bone plate is placed across the osteotomy as the tibial plateau heals in its new anatomic position.<sup>31</sup> Subsequent studies in cadaver specimens determined the final TPA should be 6.5° as rotating beyond this point results in increased strain on the CaCL.<sup>147</sup> Initial results demonstrated good-excellent functional outcome in 94% of cases.<sup>31</sup> More recent reports continue to demonstrate successful outcomes for dogs being treated with TPLO procedures for CrCL rupture.<sup>125,148</sup>

#### **6.3.5.4.3 Tibial Tuberosity Advancement (TTA):**

The TTA procedure was originally described by Montavon *et al.*<sup>149</sup> This osteotomy procedure serves to neutralize tibial thrust by advancing the tibial tuberosity to a point where the patellar ligament becomes perpendicular to a tangential line between the femoral and tibial condyles.<sup>149</sup> This results in a patellar tendon angle (PTA), which is the angle formed between the patellar ligament and tibial plateau, of 90°.<sup>149</sup> In this procedure, an osteotomy of the tibial crest is performed in the frontal plane.<sup>149</sup> The osteotomy fragment is then advanced proximally and cranially to achieve a PTA of 90°.<sup>149</sup> The tibial crest is held in this position by application of a medial bone plate that imitates a tension band.<sup>149</sup> A large retrospective study of the TTA reports similar overall complication rate to the TPLO.<sup>150</sup> Moreover, biomechanical testing of the TTA revealed that the TTA adequately restored stifle kinematics of the CrCL-deficient stifle to that of the CrCL-intact stifle by improving contact kinematics, reducing cranial tibial translation and tibial internal rotation.<sup>151</sup>

#### **6.3.5.4.4 Centers of Rotation of Angulation (CORA)-Based Leveling Osteotomy (CBLO):**

The canine tibia has a proximal curve that results in malalignment of the proximal and distal anatomic axes; therefore the canine tibia has a CORA.<sup>152</sup> By performing an osteotomy at the CORA and rotating the proximal fragment cranially, alignment of the proximal and distal anatomic axes can be achieved thereby neutralizing cranial tibial thrust.<sup>152,153</sup> The osteotomy is performed with a radial saw blade similar to a TPLO procedure, and the osteotomy is held in reduction with a bone plate and screws while the site heals.<sup>152,153</sup> In an initial case series the postoperative TPA was demonstrated to shift in 18% of cases and 8% of dogs required revision surgery.<sup>153</sup> In a subsequent study that modified the procedure by including a headless compression screw across the osteotomy site, no change in immediate postoperative TPA and final recheck TPA was observed.<sup>152</sup> Interestingly, in a population of dogs undergoing second-look arthroscopy 14 months post-CBLO, minimal progression of articular cartilage damage was observed.<sup>154</sup> It was speculated this was due to a reduction in passive laxity of tissues causing reduced cranial drawer postoperatively compared to the TPLO.<sup>154</sup>

#### 6.3.5.4.5 Triple Tibial Osteotomy (TTO):

The TTO is an osteotomy procedure that combines aspects of the TTA and CWCO.<sup>155</sup> It aims to reduce the TPA to a point where it becomes perpendicular to the patellar ligament.<sup>155</sup> Briefly, an osteotomy of the tibial crest is made in the transverse plane, followed by a second cranially based wedge osteotomy in the tibia caudal to the first osteotomy.<sup>155</sup> The wedge is removed and the caudal osteotomy is reduced.<sup>155</sup> A medially applied bone plate holds the osteotomized tibia in reduction during healing.<sup>155</sup> The original report had a 36% complication rate with fracture of the distal tibial crest osteotomy being the most common.<sup>155</sup> Although long-term owner assessment yielded a 100% owner satisfaction rate and dogs were only mildly lame, 91% of dogs had residual tibial thrust.<sup>155</sup>

### 6.4 The Lateral Suture

#### 6.4.1 Suture Material:

In the original description by DeAngelis and Lau, the lateral suture was performed using large gauge Teflon-impregnated dacron or monofilament stainless steel suture.<sup>138</sup> Flo described the use of a non-absorbable, monofilament polymerized caprolactan, and Gambardella *et al.* described the use of braided, nonabsorbable polyester.<sup>94,139</sup> Since then, several investigators have sought to describe and/or compare various materials including stainless steel, monofilament nylon and multifilament polyblend materials in order to ascertain which suture material is best for performing the lateral suture technique.<sup>156-164</sup> Nylon received attention for use as a suture material in extracapsular repair because it is a monofilament with low bacterial adherence and low plasticity.<sup>157</sup> Prior studies demonstrated a high incidence of cutaneous suture reaction and fistula formation when using braided materials.<sup>165</sup> Investigators have sought to compare nylon materials, as in fishing line versus leader line, as well as various brands for their use as a surgical prosthesis.<sup>157,160</sup> Caporn and Roe demonstrated a superiority of nylon leader line compared to nylon fishing line with regards to overall strength and less deterioration of material properties following sterilization.<sup>157</sup> Sicard *et al.* did not draw the same conclusion and found that material properties were also affected by brand, and some brands of fishing line outperformed other brands of leader line.<sup>160</sup> In both studies, it was determined that steam sterilization of nylon resulted in significant elongation compared to unsterilized nylon material, but that this could be overcome with the use of ethylene oxide sterilization methods.<sup>157,160</sup> Steam sterilization also resulted in increased diameters of nylon materials resulting in larger, less secure knot formation.<sup>157</sup> This further contributes to elongation of the tied prosthesis as the knot is expected to tighten with cyclic loading.<sup>157</sup> Nylon was also compared to other multifilament sutures in several experimental models.<sup>156,158,161,163</sup> In a biomechanical, ex-vivo comparison of four methods of extracapsular repair, a TR using Fibertape better resisted elongation compared to a lateral suture using nylon material.<sup>163</sup> The TR did not however consistently outperform other methods of extracapsular repair that also used Fibertape.<sup>163</sup> These findings are corroborated by another study that compared monofilament nylon leader line to several multifilament materials including Fibertape, FiberWire, Xen OrthoFiber and LigaFiber.<sup>161</sup> This report documented that LigaFiber had the highest strength and stiffness and least elongation of each tested materials.<sup>161</sup>

Furthermore, the braided materials consistently outperformed the nylon leader line, but it is unknown if these materials would be superior in a clinical setting since all testing was performed with the minimum load expected in a normal canine stifle.<sup>161</sup> Similar findings were found in another study.<sup>156</sup> Contrary to the aforementioned studies, Giles *et al.* found that nylon materials elongated less than multifilament FiberWire and they partially attributed this to more significant tightening of FiberWire knots.<sup>158</sup> The clinical relevance of this finding is uncertain since elongation with either material was less than 2mm.<sup>158</sup>

#### 6.4.2 Suture Securing Methods:

In addition to material types, the methods used to secure the suture used to perform extracapsular repairs has also received considerable attention.<sup>157,160,166</sup> The original description of the technique involves knotting the suture ends to form a secure mattress suture.<sup>138</sup> Since the original description, concerns have been raised within the literature with regard to decreased tensile strength of the suture material due to deformation by the knot and elongation of the suture length due to tightening of the knot that occurs with cyclic loading. This is exacerbated by the requirement to use larger gauge suture to perform the extracapsular repairs as this will result in a less secure knot.<sup>157</sup> In biomechanical testing situations, the knotted suture often failed at or near the knot.<sup>157,160,167</sup> Moreover, it was demonstrated that there is a >75% decrease in loop tension during tightening of the knot, which compromises the stability of the extracapsular repair.<sup>157</sup> Various methods of knotting suture for extracapsular repair have been investigated.<sup>167,168</sup> Dycus *et al.* compared a square knot, single self-locking knot and double self-locking knot, the latter two allow the surgeon to maintain tension during placement.<sup>167</sup> The authors found the self-locking knots had similar and higher starting tension, stiffness, and load to failure during cyclic loading compared to a square knot.<sup>167</sup> All three knot types had comparable elongation.<sup>167</sup> Additionally, clamping of the first knot in order to maintain tension during placement has not been shown to adversely affect knot strength.<sup>157,168</sup> In a separate study comparing a square knot, surgeons knot, sliding half-hitch and clamped square knot using various non-absorbable monofilament sutures, the knotting methods were found to have varying effects on the material properties of sutures depending on suture type.<sup>168</sup>

Crimping of suture is an alternative method of securing suture material used for extracapsular repair with one the main advantages being less elongation of the suture material compared to knotted samples.<sup>160,166,169</sup> Investigations of the effect of crimping versus knotting on suture strength yields contradictory results with some experiments demonstrating superior strength in crimped samples,<sup>169,170</sup> while others showed the opposite effect.<sup>156,160,166</sup> Reported modes of failure for crimped samples include slipping of suture through the crimp and breakage of suture within or near the crimp.<sup>156,166,171-173</sup> Maintenance of tension during application of crimps is also important. Moore *et al.* sought to evaluate differences manual tensioning of suture loops versus use of a tensioning device but found no difference in stiffness or ultimate load to failure between methods.<sup>174</sup>

The use of bone anchors for extracapsular stabilization was initially described by Edwards *et al.*<sup>175</sup> Use of bone anchors can help improve isometric placement of implants and avoid the need for passing of suture through osseous tunnels or around the fabella, which can lead to surgical

failure.<sup>170,176</sup> As such, the biomechanical properties of bone anchor placement in cadaver models have been investigated for use in extracapsular methods of repair.<sup>158,177</sup>

### 6.4.3 Isometry:

Isometry refers to the distance between two points remaining the same throughout motion. This is important for methods of extracapsular repair since motion at the stifle can cause relative changes in the location of suture anchoring. If the anchor sites move closer together or further apart, it can result in a lax or overtight prosthesis.<sup>170</sup> With a lax prosthesis, stifle stability cannot be maintained, and an overtight prosthesis can result in limited joint motion or failure of the construct.<sup>170</sup> Part of the difficulty in mimicking the isometry of the CrCL is that the CrCL itself is not isometric.<sup>178,179</sup> The CrCL is made of multiple fiber bands, which may be taut or lax to varying degrees throughout range of motion.<sup>178,179</sup> As a result, the CrCL can be considered quasi-isometric.<sup>179</sup> Few reports investigating isometric points for extracapsular stabilization exist and the models used to determine isometric points vary; however, there are similarities between studies.<sup>170,178,180,181</sup> A femoral anchor site as caudal as possible on the femoral condyle at the distal aspect of the lateral fabella was demonstrated to be the most isometric femoral anchor location.<sup>170,178,181</sup> Placement at this location is only possible with use of a bone anchor.<sup>170</sup> The most suitable tibial location is less consistent with recommended locations including the cranial and caudal eminences of the long digital extensor groove and the tibial tuberosity.<sup>170,178,181</sup> A study examining isometry of two tibial insertion sites, the cranial eminence of the LDE groove and the tibial tuberosity, found that placement at the tibial tuberosity better resisted cranial translation of the tibia, but placement at the LDE groove better resisted internal rotation.<sup>180</sup> This study used a circumfabellar suture as the method of femoral anchoring.<sup>180</sup> In a study by Reichert *et al.* the radiographic origin and insertions of the CrCL were determined.<sup>182</sup> Interestingly, overall the isometry of the lateral fabella as the proximal anchor point for a lateral suture was not significantly different from that of the CrCL origin when paired with several tibial anchor sites.<sup>182</sup> This was not the case when the tibial anchor site was near the cranial eminence of the LDE groove, at which point the CrCL origin was significantly more isometric than the lateral fabella.<sup>182</sup> In addition to the distance between anchor sites remaining the same throughout range of motion, another factor to consider when attempting to achieve isometry with the CrCL is tension within the suture.<sup>178</sup> As was mentioned previously, the CrCL is a complex structure with fibers variably taut and lax throughout range of motion.<sup>178,179</sup> In order to achieve complete isometry the suture material properties should also match that of the CrCL.<sup>179</sup> The difficulty in achieving this was highlighted in a study that examined tension within four variations of the lateral suture with suture tightening at varying joint angles.<sup>183</sup> In that study, no method of suture placement maintained even tension throughout range of motion.<sup>183</sup> Given the complexity of the CrCL, it is unlikely any current method of extracapsular repair will replicate the isometry of the CrCL.<sup>178</sup>

### 6.4.4 Complications:

Reports examining the rate of postoperative complications following extracapsular stabilization of the CrCL-deficient stifle are scarce.<sup>123,171,176,184</sup> Overall complication rates in one study were 15.5-17.4%.<sup>176,185</sup> Complications can be related to the prosthetic material, with papers reporting

surgical site infection, soft tissue swelling, fistulous tract formation, and premature suture failure.<sup>162,165,176,184,186</sup> The rate of fistulous tract formation using multifilament sutures is as high as 20%.<sup>165</sup> Additionally, problems can arise with suture attachment, soft tissue entrapment, avulsion of the fabella, sliding of the suture off of the fabella and bone anchor pull out.<sup>162,176,184</sup> In the study by Guenego *et al.*, 21% of patients experienced bone anchors pulling out of their insertion sites.<sup>184</sup> Additional complications include recurrent instability or altered kinematics of the stifle, post-liminary meniscal tears and peroneal nerve damage.<sup>176,184,187,188</sup>

## 7 CHAPTER II: Ruby Joint Stabilization System as an Extracapsular Method of Repair<sup>189</sup>

### 7.1 Objective:

The aim of the present study was to compare the translation and internal rotation of the CrCL-deficient stifle stabilized with the Ruby to that of the CrCL-intact and CrCL-deficient stifles. We hypothesized that the Ruby would reduce translation and internal rotation of the tibia relative to the femur, and the translation and internal rotation of the CrCL-intact and Ruby stifles would not significantly differ.

### 7.2 Materials & Methods:

#### 7.2.1 Specimen Collection and Preparation:

Twelve pelvic limbs were harvested from seven skeletally mature cadavers via disarticulation at the hip. Body weights were recorded prior to limb collection. All canines were euthanized for reasons unrelated to this study. The limbs were stored between -23°C and -20°C, and thawed at room temperature for 12-18 hours prior to testing. The skin and soft tissues from the head of the femur to the mid-metatarsals were removed, preserving the patella, patellar ligament, the medial and lateral collateral ligaments of the stifle, the medial and lateral menisci, and the cranial and caudal cruciate ligaments. The joint capsule was partially disrupted by removal of the fabellae.

#### 7.2.2 Radiographic Analysis:

Each limb was radiographed to ensure skeletal maturity and rule out the presence of pre-existing orthopedic disease.

#### 7.2.3 Ruby Procedure:

The Ruby procedure was performed in a similar manner as previously described.<sup>144</sup> The bone anchors for each test specimen were positioned at the specific anatomic locations as described below prior to motion testing of each limb. A 1.6 mm Kirschner wire (K-wire) was placed at the cranial eminence of the long digital extensor groove and advanced to exit the proximomedial aspect of the cranial tibial metaphysis. A 3.8 mm diameter cannulated drill bit was used over the previously placed K-wire to create a hole on the lateral tibial cortex. A 3.8 mm counter bore was then used to enlarge the hole to allow placement of a bone anchor. A 1.6 mm K-wire was placed in the femur, level with the distal aspect of the lateral fabella and immediately caudal to the lateral collateral ligament and was advanced towards the proximal medial femoral trochlear ridge. The appropriate UHMWPE loop length for the femoral anchor was determined by measuring the distance between the end of the tibial anchor UHMWPE loop and the femoral K-wire using a measuring device. The femoral anchor site was then created in a manner identical to the tibial anchor site. The femoral anchor with an appropriate UHMWPE loop length and titanium link size were selected to equal previously measured distance between the end of the tibial anchor UHMWPE loop and femoral anchor site. The titanium link was placed prior to

testing of the Ruby constructs and after CrCL transection. The tibia was externally rotated to reduce the distance between the UHMWPE loops and to allow successful placement of the appropriately sized titanium link. The titanium link selected achieved absence of cranial drawer without subsequent external rotation of the tibia relative to the femur.

#### 7.2.4 Testing Protocol:

To simulate the quadriceps muscle unit, a 3.0 mm hole was drilled in the centre of the patella in a cranial to caudal direction. UHMWPE fiber was passed through the hole, and the free ends were tied to form a loop, which was attached to one end of a turnbuckle. The opposite end of the turnbuckle was hooked on a 4.0 mm titanium screw placed in the proximal metaphysis of the femur. To simulate the calcaneal tendon, a 7-hole 10 ALPS plate<sup>b</sup> was secured to the caudal aspect of the calcaneus with two 2.7mm titanium screws. The most proximal hole of the plate was positioned proximal to the calcaneus to allow for attachment of a turnbuckle. A 2.0 mm metal cable was passed through the proximal eyelet of the turnbuckle, and each end of the cable was placed over a 4.0 mm titanium screw located in each of the medial and lateral fabello-femoral articular surfaces of the femur. Two 2.7 mm titanium screws were placed medially in the femur and tibia at the junctions of the proximal and middle, and middle and distal thirds of each bone to aid the use of a universal goniometer during testing to ensure consistent stifle angle.<sup>21</sup>

Each limb was placed in a custom loading frame for testing. A platform on the frame base was in contact with the paw pads and was covered with 80 grit sandpaper to provide traction during testing. An L-shaped bracket attached to a wooden block was placed on the platform and was aligned with the plantar and medial or lateral aspects of the paw to ensure consistent paw placement. The concave surface of the load cell<sup>c</sup> was located on the underside of the top portion of the loading frame. This concave surface sat on the head of the femur and allowed contact between the loading frame and limb. Relative motion between the tibia and femur was measured at stifle angles of 145°, 135°, and 125°, corresponding to the early, middle, and late stance phase of the gait cycle.<sup>190</sup> A universal goniometer was set with each arm along the anatomic long axis of the femur and tibia, along which the titanium screws were placed as a guide. Tracking receivers<sup>d</sup> were placed on the lateral aspect of the limb, one in the distal femoral metaphysis and one in the proximal tibial metaphysis (Figure 1). Each receiver was connected to the limb using two 2.0 mm titanium screws. The transmitter<sup>e</sup> for the tracking system was attached to the bar of the loading frame corresponding to the cranial aspect of and level with the stifle.

The stifle angle was set to 145° with appropriate hip and tibio-tarsal angles of 148° and 140°, respectively.<sup>190</sup> A static load of 30% of the body weight was applied to the limb to simulate normal hind limb weight bearing, and joint angles were measured a second time for accuracy. Under load, the tibia was translated caudally to collect a baseline data point. The tibia was then released, and the limb was allowed to translate and rotate under load, for which a second data

---

<sup>b</sup> KYON Veterinary Surgical Products, Zurich, Switzerland

<sup>c</sup> Transducer Techniques, Temecula, CA, USA

<sup>d</sup> FASTRAK: Polhemus, Colchester, VT, USA

<sup>e</sup> FASTRAK: Polhemus, Colchester, VT, USA

point was collected. This process was repeated until six sets of motion data were collected, and the load was removed from the limb. The stifle, hip, and hock angles were adjusted. The protocol was repeated at stifle angles of 135° and 125°. The corresponding hip and tarsal angles were 160° and 145°, and 178° and 155° respectively. A craniomedial mini-arthrotomy was performed on each stifle to facilitate transection of the CrCL. Complete transection was confirmed by the presence of cranial drawer and direct visualization. The arthrotomy was closed with 2-0 polydioxanone<sup>f</sup> in a cruciate pattern. Motion data was collected at each of the three stifle angles with the CrCL transected. The Ruby was engaged by placement of the titanium link, and motion data was collected again at each angle.

### **7.2.5 Data Collection:**

A FASTRAK<sup>g</sup> electromagnetic tracking system was used to collect motion data with six degrees of freedom for each limb in each of the described stifle conditions and stifle angles. Data were collected with regard to relative tibial and femoral translation and rotation in the following categories: cranial-caudal (Z), proximal-distal (Y), medial-lateral (X), flexion-extension (azimuth), internal-external rotation (elevation), varus-valgus (roll) (Figure 2). The transmitter was oriented with the x-axis and z-axis horizontal and the y-axis vertical.

In order to calculate relative translational and rotational data of the tibia and femur, baseline data were defined for each individual limb at each of the stifle angles and stifle conditions of interest. This was performed under the applied 30% load to be used in testing conditions. Nine sets of baseline points were collected for each limb. With the limb loaded, the tibia was translated caudally until the caudal cruciate (CaCL) was under tension, and baseline measurements were obtained. Once baseline was established and recorded, the manual tension was released and the femur and tibia were allowed to translate and rotate under 30% body weight. Relative translation and rotational (azimuth, roll, and elevation) data were calculated in reference to the specific baseline points for that particular limb at the corresponding stifle angle and stifle condition. Motion data were calculated relative to the specific baseline data for each corresponding stifle angle and stifle condition. This was done because the FASTRAK system records the motion of each receiver relative to the transmitter and not to each other. Therefore, establishing baseline data allowed for the relative motion of each receiver to be calculated under the specific testing conditions in reference to a consistent starting point (baseline). This also served as a control to ensure the limb had not significantly shifted within the loading frame between manipulations, which could introduce additional error since the femur or foot were not rigidly fixed.

### **7.2.6 Statistical Analysis:**

Standard error between baseline measurements was calculated for each individual limb at each of the stifle conditions and angles of interest. This was performed to ensure a consistent baseline was established in each loading condition. Total translation was calculated by taking the vector magnitude in the X, Y and Z planes combined. All tibial rotation data were transformed using a

---

<sup>f</sup> Ethicon, Inc., a Johnson & Johnson company, Somerville, NJ, USA

<sup>g</sup> FASTRAK: Polhemus, Colchester, VT, USA

rotation matrix to act as the zero baseline for comparison to femoral rotation. All calculations were performed in MATLAB<sup>h</sup>. Paired t-tests and standard error were used to compare the mean values for total translation, internal-external rotation, varus-valgus, and flexion-extension motion. Statistical significance was set as p-value <0.05.

### 7.3 Results

Three limbs were used to verify testing protocol. Nine limbs from five cadavers were included in the final analysis. Mean donor body weight was 25.5 +/- 3.68 kg. All limbs were skeletally mature and free of orthopedic disease based on radiographs. The measured range around each targeted stifle angle for all limbs included in the study was 125° +/- 3°, 135° +/- 3°, and 145° +/- 3°. The measured hip and tarsal angles and associated ranges at stifle angles of 125°, 135° and 145° were 146° +/- 5°, 155° +/- 5°, 180° +/- 4° for the hip, and 140° +/- 4°, 145° +/- 4°, 160° +/- 4° for the tarsus, respectively. The median and mean standard error between baseline data for translation were 0.191 mm and 0.426 mm, respectively. The median and mean standard error between baseline data for rotation were 0.321° and 0.573°, respectively. The mean +/- standard error values of total translation, internal-external rotation, varus-valgus, and flexion-extension are summarized in Table 1. P-values for comparisons between groups are summarized in Table 2.

There was a significant increase in total translation between the CrCL-intact and CrCL-deficient groups at all three stifle angles. There was a significant decrease in total translation at all stifle angles when comparing the stifles with the Ruby applied and CrCL-deficient groups. Total translation of the Ruby group was greater than the CrCL-intact group at all stifle angles, which remained significant (Figure 3).

There was a significant increase in the amount of internal rotation present between the CrCL-intact and CrCL-deficient groups at all stifle angles. The Ruby resulted in decreased internal rotation compared to the CrCL-deficient groups. This decrease was significant at stifle angles of 125° and 135°, but not at 145°. The difference in internal rotation between CrCL-intact and Ruby groups was not different at 125° and 135° but remained significantly increased in the Ruby group at 145° (Figure 4). An additional comparison of internal rotation in the CrCL-deficient stifles was performed between each of the three stifle angles due to the overall smaller magnitude of internal rotation noted at 145° compared to either 125° or 135°, this difference was not statistically significant. P-values for comparisons between 125° and 135°, 125° and 145° and 135° and 145° were 0.392, 0.065, and 0.077, respectively.

A significant increase in varus motion was seen at all stifle angles when comparing the CrCL-intact and CrCL-deficient groups. Varus motion of the Ruby group was significantly increased compared to the CrCL-intact group at all stifle angles.

### 7.4 Discussion

---

<sup>h</sup> MATLAB: The MathWorks Inc., Natick, MA, USA

The results of this study demonstrated that the Ruby reduced the total translation and internal rotation of the tibia relative to the femur when applied to the CrCL-deficient stifle under the tested loading conditions. The Ruby differed from the relative motion seen in the CrCL-intact stifle, thus rejecting the second part of our hypothesis.

Following transection of the CrCL, the range of mean increases for total translation of the tibia relative to the femur was 11.1-12.3 mm at the measured angles. This is similar to what is previously reported.<sup>34</sup> Following the Ruby, the total translation of the tibia relative to the femur was reduced, resulting in <1.2mm of difference in translation between the CrCL-intact and Ruby groups. Although this discrepancy between the CrCL-intact and Ruby groups was significant at all angles measured, the clinical relevance of this translation is unknown. A previous report of clinical cases using this implant system reported satisfactory improvements in lameness by both veterinarians and clients. To the authors' knowledge, there is no published data from which we can extrapolate to determine how this small amount of translation would affect live patients. Moreover, residual translation should be standardized against patient size as 1mm of residual translation may have a different clinical impact if it were to occur in a giant versus a toy-breed dog.

Although tibial translation does not imply meniscal translation, it could be relevant to examine the effects of this residual translation on the incidence of postliminary meniscal tears. Since normal menisci can translate up to 13 mm, investigating whether a normal meniscus could withstand this residual tibial translation would be interesting. Such conclusions are beyond the scope of this study.<sup>191</sup> Furthermore, the data collected under this testing protocol represent static loading conditions and are not representative of the complex movements of the canine stifle during the various activities of live dogs or cyclic loading over time.

Although transection of the CrCL caused a universal increase in internal tibial rotation at all three stifle angles, the smallest mean increase in internal rotation occurred at 145°, compared to 125° and 135°. Although the differences between 145° and each of the other angles was not significant, it did approach statistical significance with p-values nearing 0.05 compared to the p-value for comparing 125° and 135°, which was much larger. This difference may be explained by the lateral collateral ligament becoming more taut and resisting internal rotation of the tibia as the stifle is extended.<sup>18</sup> Tension within the lateral collateral ligament was not evaluated in this study, and therefore a definitive cause for the lesser internal rotation noted at 145° cannot be identified. Following the Ruby, the amount of internal rotation decreased to within 2.4° of the CrCL-intact stifle group for each measured angle. The amount of internal rotation present was not significantly different between the intact and the Ruby groups at angles of 125° and 135° but was significantly greater at 145°. The lack of significance between groups for internal rotation can also be due to type II error.

Previous methods of extracapsular repair have demonstrated external rotation of the tibia relative to the femur resulting from over-tightening of the prosthesis.<sup>187</sup> This external rotation of the tibia is theorized to contribute to the increased pressures within the lateral compartment of the stifle.<sup>187</sup> Over-tightening of the prosthesis is performed consciously due to the expected loosening of the material used over time as well as to mitigate cranial tibial translation. This is performed due to the perception that this is required for the surgery to be successful. The

selected titanium link that connects the femoral and tibial bone anchors minimizes the amount of internal tibial rotation without resulting in external rotation beyond what would be expected in the CrCL-intact stifle. UHMWPE loops have less elongation over time than other materials used in alternative methods of extracapsular repair, and this could be a possible benefit of the implant design that avoids increasing the pressures within the lateral compartment.<sup>192</sup> Such a conclusion is beyond the scope of static loading conditions performed in this experiment, but another study has demonstrated results that support a similar inference.<sup>159</sup>

Varus motion was increased at all stifle angles measured when comparing the CrCL-intact and CrCL-deficient groups and was subsequently reduced with the Ruby to within a mean of 2.3° of the CrCL-intact stifle. In contrast, previous studies on extracapsular repair methods reported increased pressures within the lateral compartment corresponding to increased valgus resulting from overtightening of the applied prosthesis.<sup>188</sup> The increased pressure within the lateral compartment results in articular cartilage damage and lateral meniscal tears, which are reported with an increased frequency.<sup>87,193</sup> The Ruby implant design theoretically avoids overtightening the prosthesis by selecting the link size that most closely corresponds to the remaining distance between both the tibial and femoral anchor UHMWPE loops. Choosing a link size less than the remaining distance would result in an overtight prosthesis, while choosing a link size greater than the remaining distance would result in a lax prosthesis. Selecting the appropriate link avoids increasing pressure within the lateral compartment that may increase the risk for lateral meniscal damage. However, pressures within the lateral compartment were not measured in this study, therefore conclusions about the effects of this technique in a live patient are unknown.

The pursuit of physiologic isometry is paramount in methods of extracapsular repair to avoid both laxity within the prosthesis and limited stifle motion. In this study, the Ruby was not able to duplicate normal stifle motion and this discrepancy is likely due to the difficulties in achieving physiologic isometry.<sup>170,178,180,182</sup> It is unlikely that any form of extracapsular repair will replicate the functions of the CrCL because of the complexity of its physiologic isometry.<sup>170,178</sup> In this investigation, a load was applied directly to the head of the femur instead of potting the femur in polymethyl methacrylate. We believe this method of eccentrically loading the pelvic limb allows unconstrained motion of the femur and tibia relative to one another, which better simulates normal weight-bearing of the canine limb.<sup>194</sup> This is in contrast to previously reported testing methods.<sup>143,180,195</sup>

The most significant limitations of this study are those related to study design and include the *ex vivo* conditions, which limit the ability to extrapolate these results to the Ruby *in vivo*. This is in part due to the absence of limb musculature that provides supporting structure and function to the joint beyond what was replicated in this study. Also, materials used for simulating the patellar tendon and gastrocnemius were not the same (UHMWPE vs metal cables, respectively) and could contribute unknown error to the results. The authors' reasoning for using different materials included consideration for the experimental setup. Use of a metal cable with preformed loops would have required a larger hole to be drilled through the patella and could have resulted in patellar fracture, as occurred in one of the test specimens. Additionally, the metal cables are less pliable than the UHMWPE fiber, and would have lifted the base of the patella cranially out of the trochlear groove. Metal cables were used to simulate the gastrocnemius due to ease of study design. Each cable had a preformed loop at either end that allowed equal distribution of

tension between screw heads inserted in the femur. Furthermore, the stifles used in this study were considered healthy, thus the results may not be extrapolated directly to diseased stifles and associated periarticular tissues. An additional consideration is the small number of stifles used in this study.

The authors calculated changes in relative motion of the femur and tibia by manually establishing baseline data for each limb to be tested. This method has not been previously reported and could serve to introduce error to the results if baseline data was not consistently established. In order to confirm the consistency of the baseline data, standard error measurements between baseline data points were calculated. It is important to note that any interpretation of the data in this study is limited by the standard error between baseline measurements. The mean standard error for baseline measurements was small (~0.5 mm). Additionally, measurements for this study were collected under static loading as opposed to cyclic loading, which more accurately simulates *in vivo* conditions.

## **7.5 Conclusion**

In conclusion, the Ruby resulted in reduced translation and internal rotation of the tibia relative to the femur compared to the CrCL-deficient stifle, but still differed from the CrCL-intact stifle. The differences between the Ruby and CrCL-intact groups were small, and the Ruby may result in clinically acceptable outcomes, but the effect of the residual translation and internal rotation is unknown. Additional studies evaluating the long-term clinical outcome of the Ruby are required to investigate the effects of the Ruby on the incidence of postliminary meniscal tears, maintenance of long-term stability, and progression of OA compared to traditional extracapsular techniques.

## 8 REFERENCES

1. Evans HE, de Lahunta, A.: Arthrology, in Evans HE, de Lahunta, A. (ed): *Miller's Anatomy of the Dog* (ed 4th), Vol. St. Louis, Missouri, Elsevier Saunders, 2013, pp 158-184.
2. Kowaleski MPB, R. J.; Pozzi, A.: Stifle Joint, in Johnson SAT, K. M. (ed): *Veterinary Surgery: Small Animal*, Vol 1. St. Louis, Missouri, Elsevier, 2018, pp 1071-1168.
3. Evans HE, de Lahunta, A.: The Skeleton, in Evans HE, de Lahunta, A. (ed): *Miller's Anatomy of the Dog* (ed 4th), Vol. St. Louis, Missouri, Elsevier Saunders, 2013, pp 80-157.
4. Ocal MK, Sevil-Kilimci F, Yildirim IG: Geometry of the femoral condyles in dogs. *Vet Res Commun* 36:1-6, 2012.
5. Payne JT, Constantinescu GM: Stifle Joint Anatomy and Surgical Approaches in the Dog. *Veterinary Clinics of North America: Small Animal Practice* 23:691-701, 1993.
6. Carpenter DH, Jr., Cooper RC: Mini review of canine stifle joint anatomy. *Anat Histol Embryol* 29:321-329, 2000.
7. Evans HE, de Lahunta, A., Hermanson, J. W.: The Muscular System, in Evans HE, de Lahunta, A. (ed): *Miller's Anatomy of the Dog* (ed 4th), Vol. St. Louis, Missouri, Elsevier Saunders, 2013, pp 185-280.
8. Evans HE, de Lahunta, A., Bezuidenhout, A. J.: The Heart and Arteries in Evans HE, de Lahunta, A. (ed): *Miller's Anatomy of the Dog* (ed 4th), Vol. St. Louis, Missouri, Elsevier Saunders, 2013, pp 428-504.
9. Evans HE, de Lahunta, A., Bezuidenhout, A. J.: Veins, in Evans HE, de Lahunta, A. (ed): *Miller's Anatomy of the Dog* (ed 4th), Vol. St. Louis, Missouri, Elsevier Saunders, 2013, pp 505-534.
10. Evans HE, de Lahunta, A., Bezuidenhout, A. J.: The Lymphatic System, in Evans HE, de Lahunta, A. (ed): *Miller's Anatomy of the Dog* (ed 4th), Vol. St. Louis, Missouri, Elsevier Saunders, 2013, pp 535-562.
11. Evans HE, de Lahunta, A., Kitchell, R. L.: Spinal Nerves, in Evans HE, de Lahunta, A. (ed): *Miller's Anatomy of the Dog* (ed 4th), Vol. St. Louis, Missouri, Elsevier Saunders, 2013, pp 611-657.
12. Tirgari M: The surgical significance of the blood supply of the canine stifle joint. *J Small Anim Pract* 19:451-462, 1978.
13. Arnoczky SP, Warren, R. F.: The microvasculature of the meniscus and its response to injury an experimental study in the dog. *Am J Sports Med* 11:131-141, 1983.
14. Arnoczky SP, Marshall JL: The cruciate ligaments of the canine stifle: an anatomical and functional analysis. *Am J Vet Res* 38:1807-1814, 1977.
15. Tanegashima K, Edamura K, Akita Y, et al: Functional Anatomy of the Craniomedial and Caudolateral Bundles of the Cranial Cruciate Ligament in Beagle Dogs. *Vet Comp Orthop Traumatol* 32:182-191, 2019.
16. Heffron LE, Campbell JR: Morphology, histology and functional anatomy of the canine cranial cruciate ligament. *Vet Rec* 102:280-283, 1978.
17. Yahia LH, Newman NM, St-Georges M: Innervation of the canine cruciate ligaments. A neurohistological study. *Anat Histol Embryol* 21:1-8, 1992.
18. Vasseur PB, Arnoczky SP: Collateral ligaments of the canine stifle joint: anatomic and functional analysis. *Am J Vet Res* 42:1133-1137, 1981.

19. Mann FA W-MC, Tangner CH: Manual goniometric measurement of the canine pelvic limb. *The Journal of the American Animal Hospital Association*, 1988.
20. Sabanci SS, Ocal MK: Comparison of goniometric measurements of the stifle joint in seven breeds of normal dogs. *Vet Comp Orthop Traumatol* 29:214-219, 2016.
21. Jaegger G, Marcellin-Little DJ, Levine D: Reliability of goniometry in Labrador Retrievers. *Am J Vet Res* 63:979-986, 2002.
22. Kim SE, Jones SC, Lewis DD, et al: In-vivo three-dimensional knee kinematics during daily activities in dogs. *J Orthop Res* 33:1603-1610, 2015.
23. Fischer MS, Lehmann SV, Andrada E: Three-dimensional kinematics of canine hind limbs: in vivo, biplanar, high-frequency fluoroscopic analysis of four breeds during walking and trotting. *Sci Rep* 8:16982, 2018.
24. Arnoczky SP, Torzilli, P.A., Marshall, J.L.: Biomechanical evaluation of anterior cruciate ligament repair in the dog: an analysis of the instant center of motion. *J Am Anim Hosp Assoc* 13, 1982.
25. Arnoczky SP: Pathomechanics of cruciate ligament and meniscal injuries, in Bojrab M (ed): *Disease mechanisms in small animal surgery*, Vol. Malvern, PA, Lea & Febiger, 1993.
26. Messmer MS, H.; Schawalder, P: Intraarticular measurement of forces acting on the canine medial meniscus during motion. *Vet Comp Orthop Traumatol* 13:133-138, 2001.
27. Korvick DL, Pijanowski GJ, Schaeffer DJ: Three-dimensional kinematics of the intact and cranial cruciate ligament-deficient stifle of dogs. *J Biomech* 27:77-87, 1994.
28. Tinga S, Kim SE, Banks SA, et al: Femorotibial kinematics in dogs with cranial cruciate ligament insufficiency: a three-dimensional in-vivo fluoroscopic analysis during walking. *BMC Vet Res* 14:85, 2018.
29. O'Connor BL, Visco DM, Heck DA, et al: Gait alterations in dogs after transection of the anterior cruciate ligament. *Arthritis Rheum* 32:1142-1147, 1989.
30. Slocum B, Devine T: Cranial tibial thrust: a primary force in the canine stifle. *J Am Vet Med Assoc* 183:456-459, 1983.
31. Slocum B, Slocum TD: Tibial Plateau Leveling Osteotomy for Repair of Cranial Cruciate Ligament Rupture in the Canine. *Veterinary Clinics of North America: Small Animal Practice* 23:777-795, 1993.
32. Tepic SD, D.M.; Montavon, P.M.: Biomechanics of the stifle joint, Proceedings, Proceedings of the 1st World Orthopaedic Veterinary Congress, Munich, Germany, September 10-12, 2002 (available from
33. Pozzi A, Kowaleski MP, Apelt D, et al: Effect of medial meniscal release on tibial translation after tibial plateau leveling osteotomy. *Vet Surg* 35:486-494, 2006.
34. Tashman S, Anderst W, Kolowich P, et al: Kinematics of the ACL-deficient canine knee during gait: serial changes over two years. *J Orthop Res* 22:931-941, 2004.
35. Sanchez-Bustinduy M, de Medeiros MA, Radke H, et al: Comparison of kinematic variables in defining lameness caused by naturally occurring rupture of the cranial cruciate ligament in dogs. *Vet Surg* 39:523-530, 2010.
36. DeCamp CE, Riggs CM, Olivier NB, et al: Kinematic evaluation of gait in dogs with cranial cruciate ligament rupture. *Am J Vet Res* 57:120-126, 1996.
37. Bennett D, Tennant, B., Lewis, D.G., Baughan, J., May, C., Carter, S. : A reappraisal of anterior cruciate ligament disease in the dog. *J Small Anim Pract* 29:275-297, 1988.

38. Duval JM, Budberg SC, Flo GL, et al: Breed, sex, and body weight as risk factors for rupture of the cranial cruciate ligament in young dogs. *J Am Vet Med Assoc* 215:811-814, 1999.
39. Whitehair JG, Vasseur PB, Willits NH: Epidemiology of cranial cruciate ligament rupture in dogs. *J Am Vet Med Assoc* 203:1016-1019, 1993.
40. Wilke VL, Conzemius MG, Kinghorn BP, et al: Inheritance of rupture of the cranial cruciate ligament in Newfoundlands. *J Am Vet Med Assoc* 228:61-64, 2006.
41. Witsberger TH, Villamil JA, Schultz LG, et al: Prevalence of and risk factors for hip dysplasia and cranial cruciate ligament deficiency in dogs. *J Am Vet Med Assoc* 232:1818-1824, 2008.
42. Wilke VL, Zhang S, Evans RB, et al: Identification of chromosomal regions associated with cranial cruciate ligament rupture in a population of Newfoundlands. *Am J Vet Res* 70:1013-1017, 2009.
43. Kuroki KW, N.; Ikeda, H.; Bozynski, C.C.; Leary, E.; Cook, J.L.: Histologic assessment of ligament vascularity and synovitis in dogs with cranial cruciate ligament disease. *Am J Vet Res* 80:152-158, 2019.
44. Vasseur PB, Pool RR, Arnoczky SP, et al: Correlative biomechanical and histologic study of the cranial cruciate ligament in dogs. *Am J Vet Res* 46:1842-1854, 1985.
45. Slauterbeck JR, Pankratz K, Xu KT, et al: Canine ovariohysterectomy and orchiectomy increases the prevalence of ACL injury. *Clin Orthop Relat Res*:301-305, 2004.
46. Prodromos CC, Han Y, Rogowski J, et al: A meta-analysis of the incidence of anterior cruciate ligament tears as a function of gender, sport, and a knee injury-reduction regimen. *Arthroscopy* 23:1320-1325.e1326, 2007.
47. Santarossa A, Gibson TWG, Kerr C, et al: Body composition of medium to giant breed dogs with or without cranial cruciate ligament disease. *Vet Surg*, 2020.
48. Haessig M, Bass M, Koch D, et al: Tibial tuberosity conformation as a risk factor for cranial cruciate ligament rupture in the dog. *Veterinary and Comparative Orthopaedics and Traumatology* 22:16-20, 2017.
49. Janovec J, Kyllar M, Midgley D, et al: Conformation of the proximal tibia and cranial cruciate ligament disease in small breed dogs. *Vet Comp Orthop Traumatol* 30:178-183, 2017.
50. Zeltzman PA, Pare, B., Johnson, G. M., Zeltzman, V., Robbins, M. A., Gendreau, C. L. : Relationship Between Age and Tibial Plateau Angle in Dogs With Cranial Cruciate Rupture. *J Am Anim Hosp Assoc* 41:117-120, 2005.
51. Morris E, Lipowitz, A. J.: Comparison of tibial plateau angles in dogs with and without cranial cruciate ligament injuries. *J Am Vet Med Assoc* 218, 2001.
52. Aertsens A, Rincon Alvarez J, Poncet CM, et al: Comparison of the tibia plateau angle between small and large dogs with cranial cruciate ligament disease. *Vet Comp Orthop Traumatol* 28:385-390, 2015.
53. Kyllar M, Cizek P: Cranial cruciate ligament structure in relation to the tibial plateau slope and intercondylar notch width in dogs. *J Vet Sci* 19:699-707, 2018.
54. Macias C, McKee WM, May C: Caudal proximal tibial deformity and cranial cruciate ligament rupture in small-breed dogs. *J Small Anim Pract* 43:433-438, 2002.
55. Mostafa AA, Griffon DJ, Thomas MW, et al: Morphometric characteristics of the pelvic limbs of Labrador Retrievers with and without cranial cruciate ligament deficiency. *Am J Vet Res* 70:498-507, 2009.

56. Wilke VL, Conzemius MG, Besancon MF, et al: Comparison of tibial plateau angle between clinically normal Greyhounds and Labrador Retrievers with and without rupture of the cranial cruciate ligament. *J Am Vet Med Assoc* 221:1426-1429, 2002.
57. Guénelo L, Payot M, Charru P, et al: Comparison of tibial anatomical-mechanical axis angle between predisposed dogs and dogs at low risk for cranial cruciate ligament rupture. *Vet J* 225:35-41, 2017.
58. Read RAR, G.M.: Deformity of the proximal tibia in dogs. *Vet Rec* 111:295-298, 1982.
59. Good MD, Odesten, M., Gillquist, J.: Intercondylar Notch Measurements With Special Reference to Anterior Cruciate Ligament Surgery. *Clin Orthop Relat Res* 263:185-189, 1991.
60. Witte PG: Tibial anatomy in normal small breed dogs including anisometry of various extracapsular stabilizing suture attachment sites. *Vet Comp Orthop Traumatol* 28:331-338, 2015.
61. Narama I, Masuoka-Nishiyama, M., Matsuura, T., Ozaki, K., Nagatani, M., Morishima, T. : Morphogenesis of degenerative changes predisposing dogs to rupture of the cranial cruciate ligament. *J Vet Med Sci* 58:1091-1097, 1996.
62. Comerford EJ, Innes JF, Tarlton JF, et al: Investigation of the composition, turnover, and thermal properties of ruptured cranial cruciate ligaments of dogs. *Am J Vet Res* 65:1136-1141, 2004.
63. Doom M, de Bruin T, de Rooster H, et al: Immunopathological mechanisms in dogs with rupture of the cranial cruciate ligament. *Vet Immunol Immunopathol* 125:143-161, 2008.
64. Doring AK, Junginger J, Hewicker-Trautwein M: Cruciate ligament degeneration and stifle joint synovitis in 56 dogs with intact cranial cruciate ligaments: Correlation of histological findings and numbers and phenotypes of inflammatory cells with age, body weight and breed. *Vet Immunol Immunopathol* 196:5-13, 2018.
65. Gyger O, Botteron C, Doherr M, et al: Detection and distribution of apoptotic cell death in normal and diseased canine cranial cruciate ligaments. *Vet J* 174:371-377, 2007.
66. Hayashi K, Frank JD, Dubinsky C, et al: Histologic changes in ruptured canine cranial cruciate ligament. *Vet Surg* 32:269-277, 2003.
67. Louis E, Remer KA, Doherr MG, et al: Nitric oxide and metalloproteinases in canine articular ligaments: a comparison between the cranial cruciate, the medial genual collateral and the femoral head ligament. *Vet J* 172:466-472, 2006.
68. Yarnall BW, Chamberlain CS, Hao Z, et al: Proinflammatory polarization of stifle synovial macrophages in dogs with cruciate ligament rupture. *Vet Surg* 48:1005-1012, 2019.
69. Vasseur PB, Pool, R. R., Arnoczky, S. P., Lau, R. E.: Correlative biomechanical and histologic study of the cranial cruciate ligament in dogs. *Am J Vet Res* 46:1842-1854, 1985.
70. Hayashi K, Frank JD, Hao Z, et al: Evaluation of ligament fibroblast viability in ruptured cranial cruciate ligament of dogs. *Am J Vet Res* 64:1010-1016, 2003.
71. Muir P, Schamberger GM, Manley PA, et al: Localization of cathepsin K and tartrate-resistant acid phosphatase in synovium and cranial cruciate ligament in dogs with cruciate disease. *Vet Surg* 34:239-246, 2005.
72. Kanda T, Ochi M, Ikuta Y: Adverse effects on rabbit anterior cruciate ligament after knee immobilization: changes in permeability of horseradish peroxidase. *Arch Orthop Trauma Surg* 117:307-311, 1998.

73. Flo GL: Meniscal Injuries. *Veterinary Clinics of North America: Small Animal Practice* 23:831-843, 1993.
74. Ritzo ME, Ritzo BA, Siddens AD, et al: Incidence and type of meniscal injury and associated long-term clinical outcomes in dogs treated surgically for cranial cruciate ligament disease. *Vet Surg* 43:952-958, 2014.
75. Arnault F, Cauvin E, Viguier E, et al: Diagnostic value of ultrasonography to assess stifle lesions in dogs after cranial cruciate ligament rupture: 13 cases. *Vet Comp Orthop Traumatol* 22:479-485, 2009.
76. Fazio CG, Muir P, Schaefer SL, et al: Accuracy of 3 Tesla magnetic resonance imaging using detection of fiber loss and a visual analog scale for diagnosing partial and complete cranial cruciate ligament ruptures in dogs. *Vet Radiol Ultrasound* 59:64-78, 2018.
77. Galindo-Zamora V, Dziallas P, Ludwig DC, et al: Diagnostic accuracy of a short-duration 3 Tesla magnetic resonance protocol for diagnosing stifle joint lesions in dogs with non-traumatic cranial cruciate ligament rupture. *BMC Vet Res* 9:40, 2013.
78. Plesman R, Gilbert P, Campbell J: Detection of meniscal tears by arthroscopy and arthrotomy in dogs with cranial cruciate ligament rupture: a retrospective, cohort study. *Vet Comp Orthop Traumatol* 26:42-46, 2013.
79. Pozzi A, Hildreth BE, 3rd, Rajala-Schultz PJ: Comparison of arthroscopy and arthrotomy for diagnosis of medial meniscal pathology: an ex vivo study. *Vet Surg* 37:749-755, 2008.
80. Samii VF, Dyce J, Pozzi A, et al: Computed tomographic arthrography of the stifle for detection of cranial and caudal cruciate ligament and meniscal tears in dogs. *Vet Radiol Ultrasound* 50:144-150, 2009.
81. Won WW, Lee AM, Butler JR, et al: Association of meniscal injury to joint space width on standard tibial plateau leveling osteotomy lateral radiographic projections of the canine stifle. *Vet Radiol Ultrasound* 61:16-24, 2020.
82. Gotzens B, Medl SC, Medl NS: Ex vivo cadaveric study of a laterally placed Leipzig stifle distractor for arthroscopic evaluation of the lateral meniscus in dogs. *Vet Surg* 48:O25-O33, 2019.
83. Guastella DB, Fox DB, Cook JL: Tibial plateau angle in four common canine breeds with cranial cruciate ligament rupture, and its relationship to meniscal tears. *Vet Comp Orthop Traumatol* 21:125-128, 2008.
84. Hayes GM, Langley-Hobbs SJ, Jeffery ND: Risk factors for medial meniscal injury in association with cranial cruciate ligament rupture. *Vet Surg* 39:630-634, 2010.
85. Necas A, Zatloukal J. : Factors related to the risk of meniscal injury in dogs with cranial cruciate ligament rupture. *ACTA VET BRNO* 71:77-84, 2002.
86. Kahn D, Mittelstaedt D, Matyas J, et al: Meniscus Induced Cartilaginous Damage and Non-linear Gross Anatomical Progression of Early-stage Osteoarthritis in a Canine Model. *Open Orthop J* 10:690-705, 2016.
87. Krier EM, Johnson TA, Breitenreiter AH, et al: Articular cartilage lesions associated with complete lateral meniscal tears in the dog. *Vet Surg* 47:958-962, 2018.
88. Wyland DJ, Guilak F, Elliott DM, et al: Chondropathy after meniscal tear or partial meniscectomy in a canine model. *J Orthop Res* 20:996-1002, 2002.
89. Pond MJ, Nuki, G. : Experimentally-induced osteoarthritis in the dog. *Ann Rheum Dis* 32:387-388, 1973.
90. McDevitt CA, Muir, H.: Biochemical changes in the cartilage of the knee in experimental and natural osteoarthritis in the dog. *J Bone Joint Surg* 58:94-101, 1976.

91. Widmer WR, Buckwalter, K. A., Braunstein, E. M., Hill, M. A., O'Connor, B. L., Visco, D. M.: Radiographic and magnetic resonance imaging of the stifle joint in experimental osteoarthritis of dogs. *Vet Radiol Ultrasound* 35:371-383, 1994.
92. Brandt KD, Myers, S. L., Burr, D., Albrecht, M.: Osteoarthritic changes in canine articular cartilage, subchondral bone, and synovium fifty-four months after transection of the anterior cruciate ligament. *Arthritis Rheum* 34:1560-1570, 1991.
93. Harasen G: Cranial cruciate ligament rupture in profile: 2002-2007. *CVJ* 49:193-194, 2008.
94. Gambardella PC, Wallace, L. J., Cassidy, F. : Lateral suture technique for management of anterior cruciate ligament rupture in dogs: a retrospective study. *J Am Anim Hosp Assoc* 17:33-38, 1981.
95. Johnson JM, Johnson, A. L.: Cranial cruciate ligament rupture. 1993.
96. Arnoczky S: The cruciate ligaments: the enigma of the canine stifle *Journal of Small Animal Practise* 29:71-90, 1988.
97. Slocum B, Devine, T.: Cranial tibial thrust: a primary force in the canine stifle. *J Am Vet Med Assoc* 183:456-459, 1983.
98. Henderson RA MJ: The tibial compression mechanism: a dignostic aid in stifle injuries. 1978.
99. Valen S, McCabe C, Maddock E, et al: A modified tibial compression test for the detection of meniscal injury in dogs. *58:109-114*, 2017.
100. Flo GL: Meniscal injuries and meniscal menisectomy in the canine stifle. *J Am Anim Hosp Assoc* 14:683-689, 1978.
101. Dillon DE, Gordon-Evans WJ, Griffon DJ, et al: Risk factors and diagnostic accuracy of clinical findings for meniscal disease in dogs with cranial cruciate ligament disease. *Vet Surg* 43:446-450, 2014.
102. Neal BA, Ting D, Bonczynski JJ, et al: Evaluation of meniscal click for detecting meniscal tears in stifles with cranial cruciate ligament disease. *Vet Surg* 44:191-194, 2015.
103. Gleason HE, Hudson CC, Cerroni B: Meniscal click in cranial cruciate deficient stifles as a predictor of specific meniscal pathology. *Vet Surg*, 2019.
104. Paatsama S, Sittnikow, K.: Early changes in the knee joint due to instability induced by cutting of the anterior cruciate ligament. 169-173.
105. Innes JF, Costello M, Barr FJ, et al: Radiographic progression of osteoarthritis of the canine stifle joint: a prospective study. *Vet Radiol Ultrasound* 45:143-148, 2004.
106. de Rooster H, van Bree H: Popliteal sesamoid displacement associated with cruciate rupture in the dog. *J Small Anim Pract* 40:316-318, 1999.
107. Franklin SP, Cook JL, Cook CR, et al: Comparison of ultrasonography and magnetic resonance imaging to arthroscopy for diagnosing medial meniscal lesions in dogs with cranial cruciate ligament deficiency. *J Am Vet Med Assoc* 251:71-79, 2017.
108. Tivers MS, Mahoney P, Corr SA: Canine stifle positive contrast computed tomography arthrography for assessment of caudal horn meniscal injury: a cadaver study. *Vet Surg* 37:269-277, 2008.
109. Pujol E, Van Bree H, Cauzinille L, et al: Anatomic study of the canine stifle using low-field magnetic resonance imaging (MRI) and MRI arthrography. *Vet Surg* 40:395-401, 2011.
110. Tremolada G, Winter MD, Kim SE, et al: Validation of stress magnetic resonance imaging of the canine stifle joint with and without an intact cranial cruciate ligament. *Am J Vet Res* 75:41-47, 2014.

111. Sample SJ, Racette MA, Hans EC, et al: Use of a platelet-rich plasma-collagen scaffold as a bioenhanced repair treatment for management of partial cruciate ligament rupture in dogs. *PLoS One* 13:e0197204, 2018.
112. Vasseur PB: Clinical results following nonoperative management for rupture of the cranial cruciate ligament in dogs. *Vet Surg* 13:243-246, 1984.
113. Wucherer KL, Conzemius MG, Evans R, et al: Short-term and long-term outcomes for overweight dogs with cranial cruciate ligament rupture treated surgically or nonsurgically. *J Am Vet Med Assoc* 242:1364-1372, 2013.
114. Comerford E, Forster K, Gorton K, et al: Management of cranial cruciate ligament rupture in small dogs: a questionnaire study. *Vet Comp Orthop Traumatol* 26:493-497, 2013.
115. Canapp SO, Jr., Leasure CS, Cox C, et al: Partial Cranial Cruciate Ligament Tears Treated with Stem Cell and Platelet-Rich Plasma Combination Therapy in 36 Dogs: A Retrospective Study. *Front Vet Sci* 3:112, 2016.
116. Aragon CL, Budsberg SC: Applications of Evidence-Based Medicine: Cranial Cruciate Ligament Injury Repair in the Dog. 34:93-98, 2005.
117. Bergh MS, Sullivan C, Ferrell CL, et al: Systematic review of surgical treatments for cranial cruciate ligament disease in dogs. *J Am Anim Hosp Assoc* 50:315-321, 2014.
118. Duerr FM, Martin KW, Rishniw M, et al: Treatment of canine cranial cruciate ligament disease. A survey of ACVS Diplomates and primary care veterinarians. *Vet Comp Orthop Traumatol* 27:478-483, 2014.
119. Leighton RL: Preferred method of repair of cranial cruciate ligament rupture in dogs: a survey of ACVS diplomates specializing in canine orthopedics. *American College of Veterinary Surgery. Vet Surg* 28:194, 1999.
120. von Pfeil DJF, Kowaleski MP, Glassman M, et al: Results of a survey of Veterinary Orthopedic Society members on the preferred method for treating cranial cruciate ligament rupture in dogs weighing more than 15 kilograms (33 pounds). *J Am Vet Med Assoc* 253:586-597, 2018.
121. Christopher SA, Beetem J, Cook JL: Comparison of long-term outcomes associated with three surgical techniques for treatment of cranial cruciate ligament disease in dogs. *Vet Surg* 42:329-334, 2013.
122. Conzemius MG, Evans RB, Besancon MF, et al: Effect of surgical technique on limb function after surgery for rupture of the cranial cruciate ligament in dogs. *J Am Vet Med Assoc* 226:232-236, 2005.
123. Cook JL, Luther JK, Beetem J, et al: Clinical comparison of a novel extracapsular stabilization procedure and tibial plateau leveling osteotomy for treatment of cranial cruciate ligament deficiency in dogs. *Vet Surg* 39:315-323, 2010.
124. Gordon-Evans WJ, Griffon DJ, Bubb C, et al: Comparison of lateral fabellar suture and tibial plateau leveling osteotomy techniques for treatment of dogs with cranial cruciate ligament disease. *J Am Vet Med Assoc* 243:675-680, 2013.
125. Krotscheck U, Nelson SA, Todhunter RJ, et al: Long Term Functional Outcome of Tibial Tuberosity Advancement vs. Tibial Plateau Leveling Osteotomy and Extracapsular Repair in a Heterogeneous Population of Dogs. *Vet Surg* 45:261-268, 2016.
126. Nelson SA, Krotscheck U, Rawlinson J, et al: Long-term functional outcome of tibial plateau leveling osteotomy versus extracapsular repair in a heterogeneous population of dogs. *Vet Surg* 42:38-50, 2013.

127. Au KK, Gordon-Evans WJ, Dunning D, et al: Comparison of short- and long-term function and radiographic osteoarthritis in dogs after postoperative physical rehabilitation and tibial plateau leveling osteotomy or lateral fabellar suture stabilization. *Vet Surg* 39:173-180, 2010.
128. Paatsama S: Ligament injuries in the canine stifle joint: a clinical and experimental study. Royal Veterinary College, 1952.
129. Shires PK: Intracapsular repairs for cranial cruciate ligament ruptures. *Vet Clin North Am Small Anim Pract* 23:761-776, 1993.
130. Arnoczky SP, Tarvin, G. B., Marshall, J. L., Saltzman, B.: Over-the-top procedure - technique for anterior cruciate ligament substitution in the dog. *J Am Vet Med Assoc* 15:283-290, 1979.
131. Shires PK, Hulse, D. A., Liu, W.: The under-and-over fasdal replacement technique for anterior cruciate ligament rupture in dogs: A retrospective study. *J Am Anim Hosp Assoc* 20:69-77, 1984.
132. Denny HR, Barr, A. R. S.: An evaluation of two "over-the-top" techniques for anterior cruciate ligament replacement in the dog. *J Small Anim Pract* 25:759-769, 1984.
133. Lopez MJ, Markel MD, Kalscheur V, et al: Hamstring graft technique for stabilization of canine cranial cruciate ligament deficient stifles. *Vet Surg* 32:390-401, 2003.
134. Barnhart MD, Maritato K, Schankereli K, et al: Evaluation of an intra-articular synthetic ligament for treatment of cranial cruciate ligament disease in dogs: a six-month prospective clinical trial. *Vet Comp Orthop Traumatol* 29:491-498, 2016.
135. Barnhart MD, Bufkin BW, Litsky AS: Biomechanical Comparison of Four Methods of Fixation of a Polymeric Cranial Cruciate Ligament in the Canine Femur and Tibia. *Vet Comp Orthop Traumatol* 32:112-116, 2019.
136. Childers HE: New methods for cruciate ligament repair. *Mod Vet Prac* 47:59-60, 1966.
137. Pearson PT: The canine stifle joint. *Proceedings of the 36th Annual Meeting of the American Animal Hospital Association*:397-404, 1969.
138. DeAngelis M, Lau, R.E.: A lateral retinacular imbrication technique for the surgical correction of anterior cruciate ligament rupture in the dog. *J Am Vet Med Assoc* 157:79-84, 1970.
139. Flo GL: A modification of the lateral retinacular imbrication technique for stabilizing cruciate ligament injuries. *J Am Anim Hosp Assoc* 11:570-576, 1975.
140. Piermattei DL, Flo, G. L., DeCamp, C. E. : The Stifle Joint, in Piermattei DL, Flo, G. L., DeCamp, C. E. (ed): *Brinker, Piermattei, and Flo's Handbook of Small Animal Orthopedics and Fracture Repair* (ed 4th), Vol. St. Louis, Missouri, Saunders Elsevier, 2006, pp 562-632.
141. Smith GK, Torg, J.S.: Fibular head transposition for repair of cruciate-deficient stifle in the dog. *J Am Vet Med Assoc* 187:375-383, 1985.
142. Monnet E, Schwarz, P. D., Powers, B.: Popliteal tendon transposition for stabilization of the cranial cruciate ligament deficient stifle joint in dogs: an experimental study. *Vet Surg* 24:465-475, 1995.
143. D'Amico LL, Lanz OI, Aulakh KS, et al: The effects of a novel lateral extracapsular suture system on the kinematics of the cranial cruciate deficient canine stifle. *Vet Comp Orthop Traumatol* 26:271-279, 2013.
144. Muro NM, Lanz OI: Use of a novel extracapsular bone anchor system for stabilisation of cranial cruciate ligament insufficiency. *J Small Anim Pract* 58:284-292, 2017.

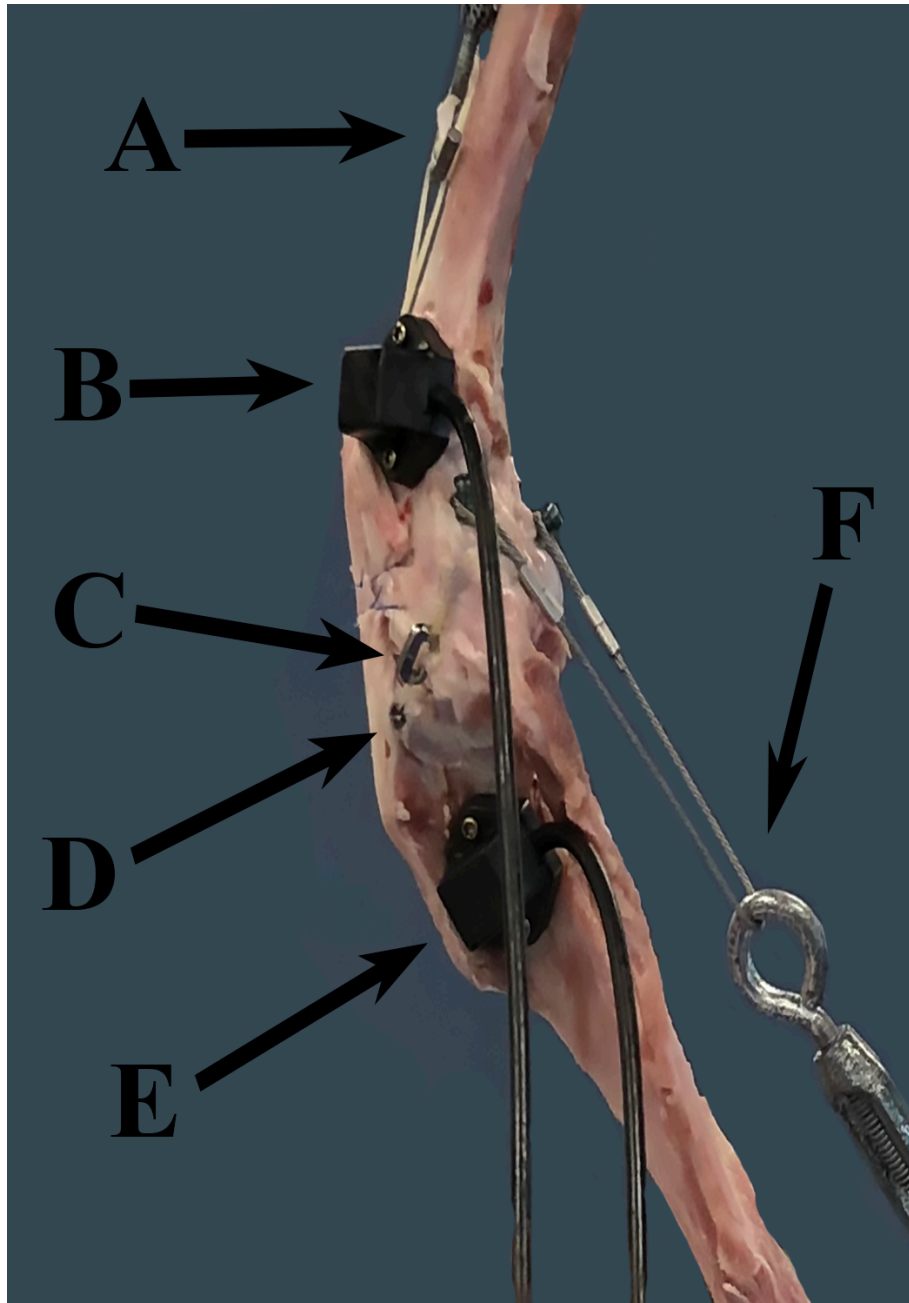
145. Slocum B, Devine T: Cranial tibial wedge osteotomy: a technique for eliminating cranial tibial thrust in cranial cruciate ligament repair. *J Am Vet Med Assoc* 184:564-569, 1984.
146. Oxley B, Gemmill TJ, Renwick AR, et al: Comparison of complication rates and clinical outcome between tibial plateau leveling osteotomy and a modified cranial closing wedge osteotomy for treatment of cranial cruciate ligament disease in dogs. *Vet Surg* 42:739-750, 2013.
147. Warzee CC, Dejardin LM, Arnoczky SP, et al: Effect of tibial plateau leveling on cranial and caudal tibial thrusts in canine cranial cruciate[ndash ]deficient stifles: An in vitro experimental study. *Veterinary Surgery* 30:278-286, 2001.
148. Shimada M, Mizokami N, Ichinohe T, et al: Long-term outcome and progression of osteoarthritis in uncomplicated cases of cranial cruciate ligament rupture treated by tibial plateau leveling osteotomy in dogs. *J Vet Med Sci* 82:908-916, 2020.
149. Montavon PM, Damur, D. M., Tepic, S. : Advancement of the tibial tuberosity for the treatment of cranial cruciate deficient canine stifle, Proceedings, Proceedings of the 1st World Orthopedic Veterinary Congress, Munich, Germany, September 5-8, 2002 (available from
150. Wolf RE, Scavelli TD, Hoelzler MG, et al: Surgical and postoperative complications associated with tibial tuberosity advancement for cranial cruciate ligament rupture in dogs: 458 cases (2007-2009). *J Am Vet Med Assoc* 240:1481-1487, 2012.
151. Kim SE, Pozzi A, Banks SA, et al: Effect of tibial tuberosity advancement on femorotibial contact mechanics and stifle kinematics. *Vet Surg* 38:33-39, 2009.
152. Raske M, Hulse D, Beale B, et al: Stabilization of the CORA based leveling osteotomy for treatment of cranial cruciate ligament injury using a bone plate augmented with a headless compression screw. *Vet Surg* 42:759-764, 2013.
153. Hulse D, Beale B., Kowaleski, M. : CORA based leveling osteotomy for treatment of the CCL deficient stifle, Bologna, Italy, 2010 (available from
154. Vasquez B, Hulse D, Beale B, et al: Second-look arthroscopic findings after CORA-based leveling osteotomy. *Vet Surg* 47:261-266, 2018.
155. Bruce WJ, Rose A, Tuke J, et al: Evaluation of the triple tibial osteotomy. A new technique for the management of the canine cruciate-deficient stifle. *Vet Comp Orthop Traumatol* 20:159-168, 2007.
156. Burgess R, Elder S, McLaughlin R, et al: In vitro biomechanical evaluation and comparison of FiberWire, FiberTape, OrthoFiber, and nylon leader line for potential use during extraarticular stabilization of canine cruciate deficient stifles. *Vet Surg* 39:208-215, 2010.
157. Caporn T, Roe S: Biomechanical evaluation of the suitability of monofilament nylon fishing and leader line for extra-articular stabilisation of the canine cruciate-deficient stifle. 9:126-133, 1996.
158. Giles JT, 3rd, Coker D, Rochat MC, et al: Biomechanical analysis of suture anchors and suture materials in the canine femur. *Vet Surg* 37:12-21, 2008.
159. S BST: Combined Fatigue and Wear Testing of Anchored Sutures, in Orthopaedic Research Society, Vol. New Orleans 2018.
160. Sicard GK, Hayashi K, Manley PA: Evaluation of 5 types of fishing material, 2 sterilization methods, and a crimp-clamp system for extra-articular stabilization of the canine stifle joint. *Vet Surg* 31:78-84, 2002.

161. Rose ND, Goerke D, Evans RB, et al: Mechanical testing of orthopedic suture material used for extra-articular stabilization of canine cruciate ligament-deficient stifles. *Vet Surg* 41:266-272, 2012.
162. Stork CK, Owen, M. R., Li, A., Schwarz, T., Bennett, D., Carmichael, S.: Radiographic features of a lateral extracapsular wire suture in the canine cranial cruciate deficient stifle. *J Small Anim Pract* 42:487-490, 2001.
163. Choate CJ, Lewis DD, Conrad BP, et al: Assessment of the craniocaudal stability of four extracapsular stabilization techniques during two cyclic loading protocols: a cadaver study. *Vet Surg* 42:853-859, 2013.
164. Olmstead ML: The use of orthopedic wire as a lateral suture for stifle stabilization. *Vet Clin North Am Small Anim Pract* 23:735-753, 1993.
165. Dulisch M: Suture reaction following extra-articular stifle stabilization in the dog. *J Am Anim Hosp Assoc* 17:569-571, 1981.
166. Vianna ML, Roe SC: Mechanical comparison of two knots and two crimp systems for securing nylon line used for extra-articular stabilization of the canine stifle. *Vet Surg* 35:567-572, 2006.
167. Dycus DL, Wardlaw, J. L., Rowe, D., Elder, S. : In-vitro comparison of 3 knotting techniques for lateral fabellotibial suture stabilization. *Can J Vet* 54:353-358, 2013.
168. Huber DJ, Egger, E. L., James, S. P.: The effect of knotting method on the structural properties of large diameter nonabsorbable monofilament sutures. *Vet Surg* 28:260-267, 1999.
169. Anderson CC, 3rd, Tomlinson JL, Daly WR, et al: Biomechanical evaluation of a crimp clamp system for loop fixation of monofilament nylon leader material used for stabilization of the canine stifle joint. *Vet Surg* 27:533-539, 1998.
170. Roe SC, Kue J, Gemma J: Isometry of potential suture attachment sites for the cranial cruciate ligament deficient canine stifle. *Vet Comp Orthop Traumatol* 21:215-220, 2008.
171. McCartney WT, O'Connor, J. V., McCann, W. M.: Incidence of infection and premature crimp failure after repair of cranial cruciate ligament-deficient stifles in 110 dogs. *Vet Rec* 161:232-233, 2007.
172. Moores AP, Beck AL, Jespers KJ, et al: Mechanical evaluation of two crimp clamp systems for extracapsular stabilization of the cranial cruciate ligament-deficient canine stifle. *Vet Surg* 35:470-475, 2006.
173. Langley-Hobbs SJ, Sutcliffe MPF, Cutting ED, et al: A biomechanical comparison of six different double loop configurations for use in the lateral fabella suture technique. *Veterinary and Comparative Orthopaedics and Traumatology* 21:391-399, 2017.
174. Moores AP, Beck AL, Jespers KJ, et al: Mechanical evaluation of two loop tensioning methods for crimp clamp extracapsular stabilization of the cranial cruciate ligament-deficient canine stifle. *Vet Surg* 35:476-479, 2006.
175. Edwards MR, Taylor, R. A., Franceschi, R. A.: Clinical Case Applications of Mitek Tissue Anchors in Veterinary Orthopaedics. *Vet Comp Orthop Traumatol* 6:208-212, 1993.
176. Casale SA, McCarthy RJ: Complications associated with lateral fabellotibial suture surgery for cranial cruciate ligament injury in dogs: 363 cases (1997-2005). *J Am Vet Med Assoc* 234:229-235, 2009.
177. Roca RY, Peura A, Kowaleski MP, et al: Ex vivo mechanical properties of a 2.5-mm bone anchor for treatment of cranial cruciate ligament rupture in toy breed dogs. *Vet Surg* 49:736-740, 2020.

178. Hulse D, Hyman W, Beale B, et al: Determination of isometric points for placement of a lateral suture in treatment of the cranial cruciate ligament deficient stifle. *Vet Comp Orthop Traumatol* 23:163-167, 2010.
179. Roe SC: The challenge of isometry for extracapsular devices. *Vet Comp Orthop Traumatol* 26:VII, 2013.
180. Aulakh KS, Harper TA, Lanz OI, et al: Effect of tibial insertion site for lateral suture stabilization on the kinematics of the cranial cruciate ligament deficient-stifle during early, middle and late stance: an in vitro study. *Vet Comp Orthop Traumatol* 26:208-217, 2013.
181. Hyman W, Hulse, D., Saunders, B: Strain analysis of femoral and tibial anchorage sites for extraarticular reconstruction of the cranial cruciate deficient stifle joint, Proceedings, 28th VOS Meeting, Chateau Lake Louise, Canada, 2001 (available from
182. Reichert EE, Kunkel KA, Suber JT, et al: Radiographic localization and isometry of the origin and insertion of the canine cranial cruciate ligament. *Vet Surg* 42:860-866, 2013.
183. Fischer C, Cherres M, Grevel V, et al: Effects of attachment sites and joint angle at the time of lateral suture fixation on tension in the suture for stabilization of the cranial cruciate ligament deficient stifle in dogs. *Vet Surg* 39:334-342, 2010.
184. Guenego L, Zahra A, Madelenat A, et al: Cranial cruciate ligament rupture in large and giant dogs. A retrospective evaluation of a modified lateral extracapsular stabilization. *Vet Comp Orthop Traumatol* 20:43-50, 2007.
185. Levien AS, Brodbelt DC, Arthurs GI: Retrospective analysis of complications and outcomes in Boxers and Staffordshire Bull Terriers undergoing cranial cruciate ligament surgery. *Aust Vet J* 91:220-225, 2013.
186. Meyer DC, Nyffeler RW, Fucentese SF, et al: Failure of suture material at suture anchor eyelets. *Arthroscopy* 18:1013-1019, 2002.
187. Chailleux N, Lussier B, De Guise J, et al: In vitro 3-dimensional kinematic evaluation of 2 corrective operations for cranial cruciate ligament-deficient stifle. *Can J Vet Res* 71:175-180, 2007.
188. Tonks CA, Pozzi A, Ling HY, et al: The effects of extra-articular suture tension on contact mechanics of the lateral compartment of cadaveric stifles treated with the TightRope CCL or lateral suture technique. *Vet Surg* 39:343-349, 2010.
189. Dominic C, Lanz OI, Muro N, et al: Titanium-Alloy Anchoring System as a Suitable Method of Extracapsular Repair. *Front Vet Sci* 7:592742, 2020.
190. Hottinger HA, DeCamp CE, Olivier NB, et al: Noninvasive kinematic analysis of the walk in healthy large-breed dogs. *Am J Vet Res* 57:381-388, 1996.
191. Park BH, Banks SA, Pozzi A: Quantifying meniscal kinematics in dogs. *J Orthop Res* 36:1710-1716, 2018.
192. A B: Handbook of Tensile Properties of Textile and Technical Fibers in The Manufacture, Properties and Applications of High Strength, High Modulus Polyethylene Fibers Vol. Florida, CRC Press LCC, 2009, pp 437-485.
193. Ralphs SC, Whitney WO: Arthroscopic evaluation of menisci in dogs with cranial cruciate ligament injuries: 100 cases (1999-2000). *J Am Vet Med Assoc* 221:1601-1604, 2002.
194. Fu YC, Torres BT, Budsberg SC: Evaluation of a three-dimensional kinematic model for canine gait analysis. *Am J Vet Res* 71:1118-1122, 2010.

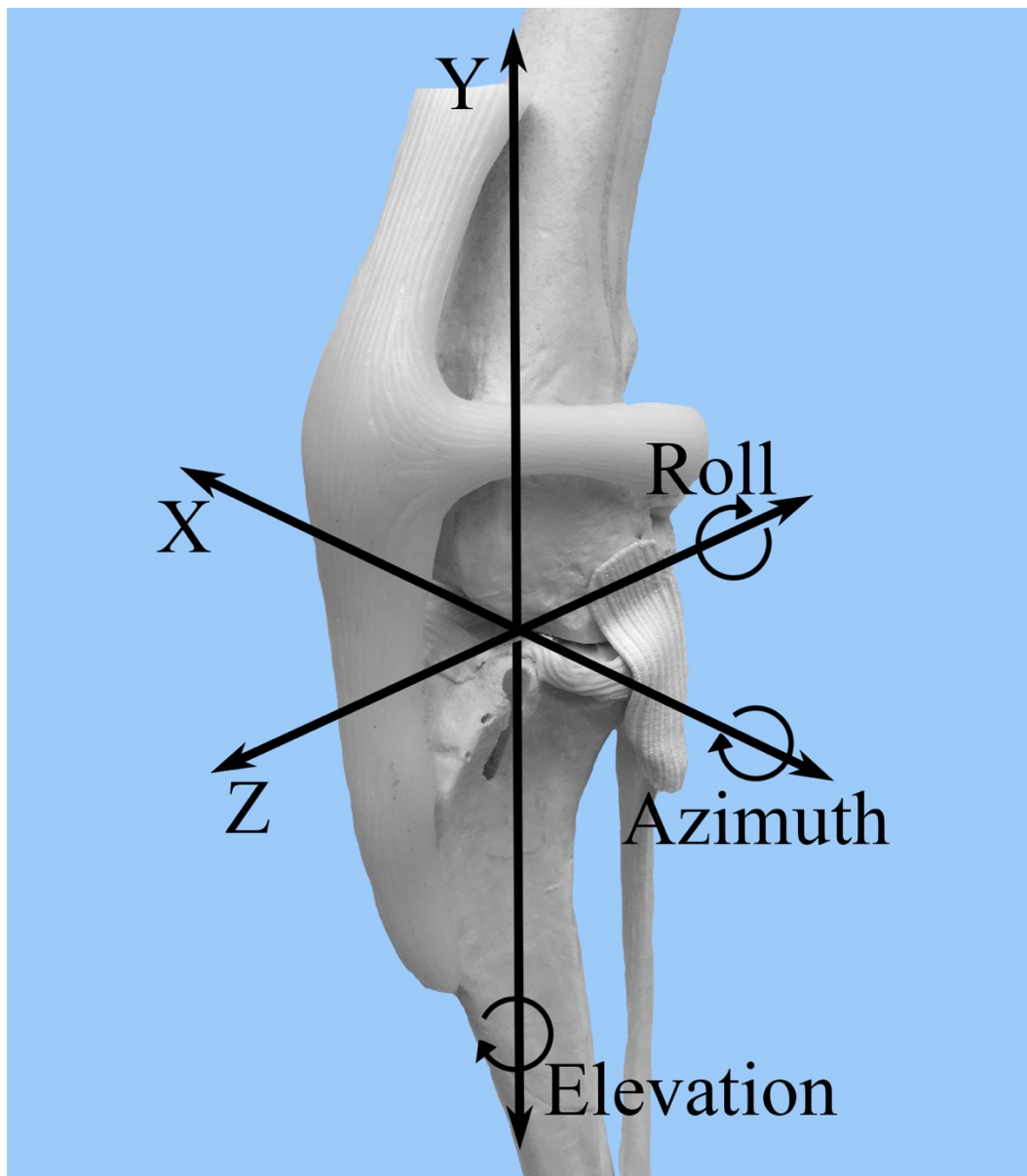
195. Butler JR, Syrcle JA, McLaughlin RM, et al: The effect of tibial tuberosity advancement and meniscal release on kinematics of the cranial cruciate ligament-deficient stifle during early, middle, and late stance. *Vet Comp Orthop Traumatol* 24:342-349, 2011.

Figure 1: FASTRAK receivers and Ruby implants. This figure demonstrates the location of the FASTRAK receivers and Ruby implants, which were applied to the lateral aspect of the stifle in each specimen. A = turnbuckle and UHMWPE simulating the quadriceps unit, B = the femoral FASTRAK receiver, C = the titanium link of the Ruby, D = the tibial anchor of the Ruby, E = the tibial FASTRAK receiver, F = the turnbuckle and metal cable simulating the calcaneal tendon. Note: the femoral Ruby bone anchor is not visible through the soft tissues in this photo.



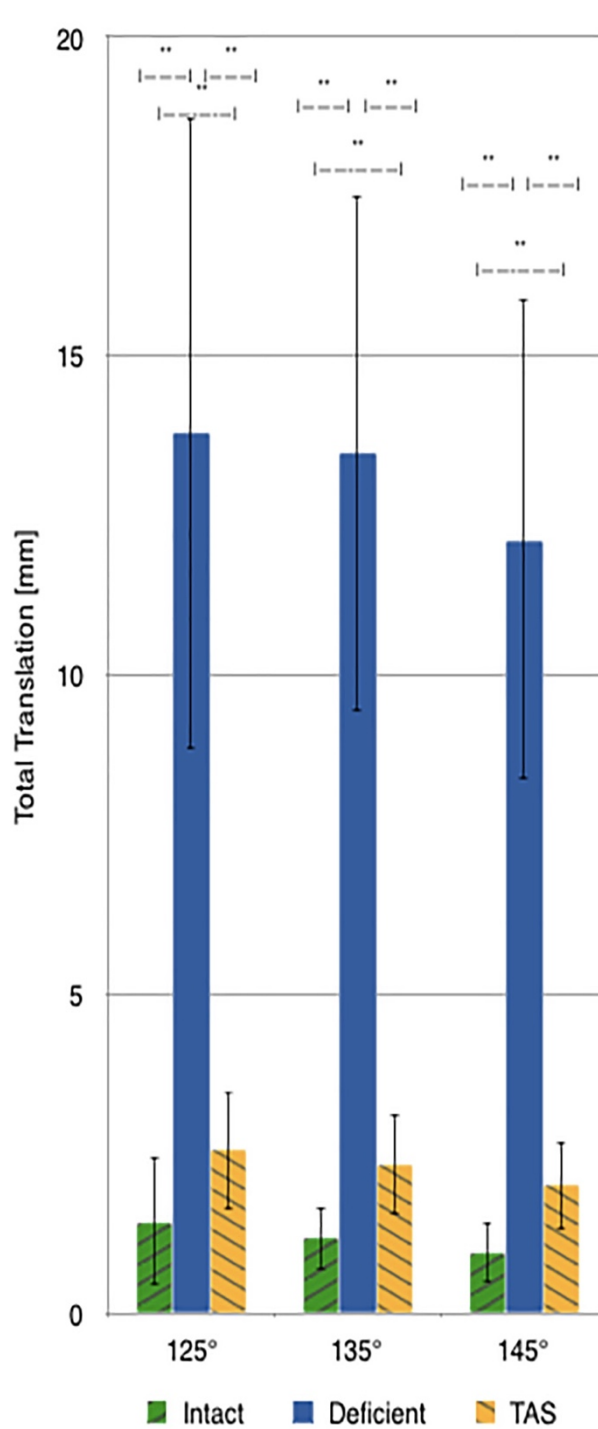
## 10 APPENDIX B<sup>189</sup>

Figure 2: FASTRAK coordinate system. A craniolateral view of the canine stifle is shown with the superimposed coordinate system that corresponds to the direction of stifle motion detected by the FASTRAK Tracking System. Z = cranial-caudal; Y = proximal-distal; X = medial-lateral; Azimuth = flexion-extension; Elevation = internal-external rotation; Roll = varus-valgus.



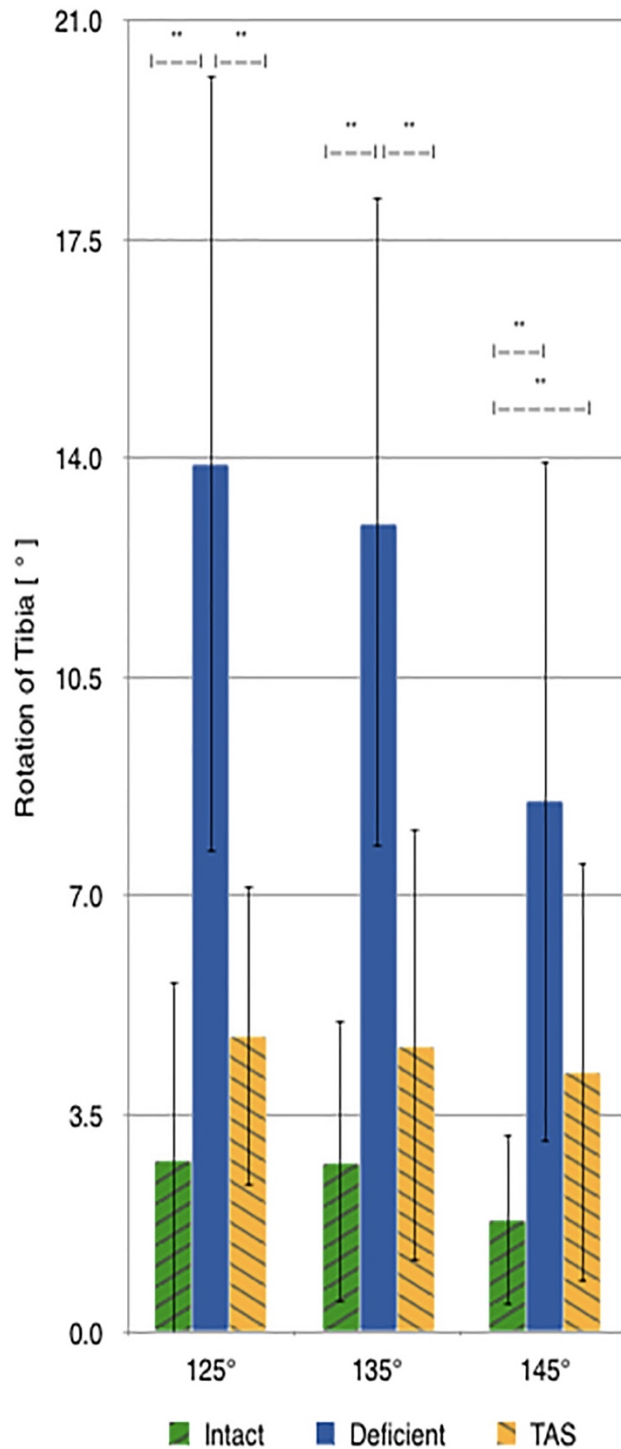
11 APPENDIX C<sup>189</sup>

Figure 3: Mean values of total translation with the standard deviation bars applied. Comparisons between two groups that are significantly different from one another are indicated with a horizontal bar and double asterisks.



12 APPENDIX D<sup>189</sup>

Figure 4: Mean values of internal-external rotation with the standard deviation bars applied. Comparisons between two groups that are significantly different from one another are indicated with a horizontal bar and double asterisks.



### 13 APPENDIX E<sup>189</sup>

Table 1: Mean +/- standard error values for total translation, internal rotation, varus and flexion. Total translation is measured in mm, internal rotation, varus and flexion are measured in degrees. CrCL = cranial cruciate ligament.

	STIFLE CONDITION	125°	135°	145°
TOTAL TRANSLATION (mm)	CrCL-INTACT	1.459 ± 0.338	1.187 ± 0.165	0.970 ± 0.156
	CrCL-DEFICIENT	13.798 ± 1.651	13.488 ± 1.343	12.136 ± 1.259
	Ruby	2.565 ± 0.303	2.341 ± 0.262	2.019 ± 0.233
INTERNAL ROTATION (degrees)	CrCL-INTACT	2.769 ± 0.949	2.733 ± 0.757	1.816 ± 0.457
	CrCL-DEFICIENT	13.920 ± 2.073	12.966 ± 1.731	8.503 ± 1.816
	Ruby	4.746 ± 0.805	4.586 ± 1.154	4.160 ± 1.116
VARUS (degrees)	CrCL-INTACT	1.100 ± 0.331	0.744 ± 0.181	0.661 ± 0.245
	CrCL-DEFICIENT	5.517 ± 1.059	4.406 ± 0.907	4.094 ± 0.953
	Ruby	3.351 ± 0.630	3.036 ± 0.497	1.998 ± 0.324
FLEXION (degrees)	CrCL-INTACT	0.491 ± 0.185	0.338 ± 0.064	0.496 ± 0.191
	CrCL-DEFICIENT	3.054 ± 0.895	3.392 ± 0.808	3.380 ± 0.588
	Ruby	1.180 ± 0.223	0.870 ± 0.238	0.881 ± 0.143

## 14 APPENDIX F<sup>189</sup>

Table 2: Summarized p-values for differences in total translation, internal rotation, varus and flexion between groups. Statistical significance was set at <0.05. CrCL = cranial cruciate ligament. \* = marks a significant test result.

	STIFLE CONDITION	125°	135°	145°
TOTAL TRANSLATION	CrCL-INTACT – CrCL-DEFICIENT	0.00007*	0.00002*	0.00002*
	CrCL-DEFICIENT – Ruby	0.00005*	0.00001*	0.00002*
	CrCL-INTACT – Ruby	0.02065*	0.00457*	0.00262*
INTERNAL ROTATION	CrCL-INTACT – CrCL-DEFICIENT	0.002*	0.001*	0.004*
	CrCL-DEFICIENT – Ruby	0.003*	0.003*	0.067
	CrCL-INTACT – Ruby	0.146	0.083	0.036*
VARUS	CrCL-INTACT – CrCL-DEFICIENT	0.005*	0.004*	0.011*
	CrCL-DEFICIENT – Ruby	0.162	0.316	0.085
	CrCL-INTACT – Ruby	0.011*	0.002*	0.005*
FLEXION	CrCL-INTACT – CrCL-DEFICIENT	0.029*	0.005*	0.001*
	CrCL-DEFICIENT – Ruby	0.087	0.022*	0.003*
	CrCL-INTACT – Ruby	0.094	0.057	0.011*